Urban Climate News

Quarterly Newsletter of the IAUC

ISSUE NO. 71 MARCH 2019 • www.urban-climate.org • INTERNATIONAL ASSOCIATION FOR URBAN CLIMATE

From the IAUC President

It has been a significant three months for the IAUC, with much to report in *Urban Climate News*. Thanks once again to David Pearlmutter for his efforts in bringing this newsletter together.

I begin this column whilst in Marrekesh, Morocco, where I am attending the Joint Panel Meeting of GCOS (Global Climate Observation System – set up by WMO/UNFCCC back in the early 90's to provide data inputs to the deliberations of the IPCC). I Co-Chair the Terrestrial Observations Panel for Climate (there is also an ocean and atmospheric panel) that traditionally has provided information on terrestrial variables (so-called Essential Climate Variables) such as albedo, snow/ice cover, land use/land cover, etc., mainly to the modelling community of IPCC WG1. Following the Paris Agreement, there is an increasing call on GCOS to provide information in support of impacts, adaptation and mitigation (the domains of WG2 and WG3). There is huge scope for urban climate adaptation to become an important part of our reporting – more about that in a later column.

I am very pleased to report to the membership the establishment of a new Treasurer position as part of the IAUC Executive. The new Treasurer is Ariane Middel (Arizona State University) who is gradually assuming responsibilities from Gerald Mills (University College Dublin). Gerald has done a wonderful job over many years looking after the IAUC finances in a rather informal capacity, and the Board of the IAUC sincerely thanks Gerald for his efforts. Relevant details of changes to the administrative arrangements can be found at http://www.urban-climate.org/organisation/iauc-procedures-and-administrative-matters/.

The long process of deciding on the location of our next conference has now come to completion, with the long-anticipated announcement in this newsletter of **Sydney as the venue for ICUC-11 in 2021**. I want to thank all the candidate cities for their efforts in putting forward their venues, along with members of the Board and the IAUC Executive (especially Andreas Christen and Ariane Middel) for an excellent engagement process with the membership that has finally led to the selection of Sydney, that will make a wonderful host city. More details on ICUC-11 follow below.

Finally, I note again the sad passing in Israel of Professor Arieh Bitan, a most distinguished member of the urban climate community, and a past recipient of the Luke Howard Award. Hadas Saaroni has provided a moving tribute to Professor Bitan in this newsletter.

– Nigel Tapper,
IAUC President
nigel.tapper@monash.edu

Inside the March issue...

School climate strikes draw thousands to the streets in cities around the globe

March 15, 2019 — A movement that began with a single teenager protesting outside the Swedish parliament last summer became a global phenomenon Friday, as hundreds of thousands of students worldwide skipped school and took to the streets to demand urgent action on climate change.

Starting in the South Pacific and moving west with the sun, the protests blanketed grand city centers and humble village squares, national parliament buildings and tiny town halls. The demonstrations stretched to every continent, across more than 100 countries and 1,700 locations, from India to South Africa to Greenland.

The coordinated demonstrations were planned as the largest manifestation to date of the Fridays for Future movement, in which students forgo classes each week in favor of something they have said is more important: pleading for action on an issue that will affect every person on the planet, but young people most of all.

"You're stealing our future!" a crowd of some 20,000 demonstrators chanted Friday outside the German government ministry in Berlin.

The adults most responsible for the ravages of climate change "are going to be gone soon enough," said 14-year-old Ashton Cassa, who was on the streets of Sydney on Friday with an estimated 30,000 other Australians. "It is up to us kids to make a difference."

In New York, so many young protesters gathered outside city hall, chanting and pumping their fists, that they spilled into the nearby bike lane and street.

"Climate change is not a lie," they chanted. "We won't let our planet die."

Camilo Budet, a 5-year-old kindergartner from Brooklyn, came with his mother. He carried a sign almost as large as he was, which read, "Stop polluting now."

Peter Yarrow, of the 1960s folk trio folk trio Peter, Paul and Mary, led the group in a song. "Let the children lead," he said, as the young crowd echoed him. "That's what we need."

In Montreal, a crowd of several thousand young people gathered at a park near McGill University before marching downtown. Some students drummed or blew air horns, and marchers of all ages carried homemade signs, most written in French.

"The future belongs to us," said Federico Mazziotti, 25, a student at one of Quebec's state universities.

In San Francisco, middle and high school students from around the Bay Area filled a downtown plaza. "Ain't no power like the power of the youth, cause the power of the youth don't stop!" they chanted in unison.

"Everyone thinks that education comes first, and education is really important, but this is important, too," said Kristen Khyzoma, 16, who left during her second period class Friday.

Students call for climate action in Kampala, Uganda. ***Source:*** washingtonpost.com

On a springlike day in Washington, groups of friends and schoolmates began assembling on the Capitol lawn about 11:30 a.m. They brought giant beach balls to bounce around the crowd and wands to blow soap bubbles. Some lounged on multicolored parachutes the organizers had set up on the grass.

"There are people in that building who are leaving behind a mess for us, for our generation to clean up," 13-year-old Arkadi Vidales said, gesturing to the Capitol dome. "We need to do something about it — now."

Despite their frustration, the protesters across the globe Friday delivered their dire messages in a largely peaceful way, but also with exasperation and a sense of urgency.

U.N. researchers have said the world has only the next dozen years to sharply curb carbon dioxide emissions and head off the more catastrophic impacts of climate change, such as rising seas that inundate cities, crop failures that spawn famines and more severe weather-related disasters that ravage communities and cause billions of dollars in damage.

But politicians remain far apart in their efforts to address global warming. President Trump has vowed to withdraw the United States from an international climate accord signed in 2015. And many countries that remain are far from meeting their pledges to reduce carbon emissions.

"Since our leaders are behaving like children, we will have to take the responsibility they should have taken long ago," Greta Thunberg, the Swedish teen who launched the movement, told a U.N. climate gathering in December in a speech that, with equal parts clarity and audacity, rocketed her to fame.

"I don't want your hope," Thunberg told the world's elite at an economic forum in Davos a month later. "I want you to panic."

The 16-year-old, who started protesting by herself in Stockholm, has inspired young people around the world to follow her example. Protests have been especially large in European capitals, but Friday's demonstrations included large gatherings in nearly every corner of the globe.

"The first day I sat, I was all alone," Thunberg has said. Now, "it's amazing to talk to these people who are doing the same thing and fighting for the same cause... all around the world." Parents, educators and other adults also joined the throngs of student protesters Friday.

In Washington, Adam Siegel came to the strike with his 14-year-old daughter, Leah, a student at McLean High School. "This is a form of education," he said. "This is civil action... This is citizenship."

The young people behind the strikes leveraged the power of social media to plan and organize the worldwide rallies, and on Friday they enthusiastically marched on the front lines, bullhorns in hand.

An estimated 150,000 people turned out in dozens of demonstrations across Australia. Somewhat smaller protests unfolded in cities across Asia. In Europe, capitals such as Berlin, Paris and London were filled with placard-wielding students who had packed into trains and subways to reach the demonstrations. Tens of thousands of people were estimated to have turned out in each of those cities.

Large groups also turned out in New York, Washington and some other U.S. cities in roughly three dozen U.S. states. Some said the demonstrations have become so popular that to be in school on a Friday during a protest was the exception, not the norm. "The last time, only four people were left in class, and I didn't want to be one of them," said 18-year-old Berlin resident Enrico Csonka.

In Paris, the march started at the Place du Pantheon, the site of the French Republic's mausoleum for its most cherished citizens. The students climbed atop bus stations, hung onto streetlights and chanted: "One, two, three degrees. It's a crime against humanity."

A large, boisterous crowd — chanting, "Solutions, not pollution" — marched through central London, weaving by landmarks such as Downing Street and Buckingham Palace.

Friday marked 13-year-old Alexandria Villasenor's 14th week striking in front of the United Nations headquarters in New York. Since December, she had sat there mostly alone through rain, snow and the polar vortex.

On Friday, she wasn't alone anymore.

"Today, we are declaring the era of American climate change denialism over," she declared to the morning's crowd outside the United Nations.

For all the urgency and fervor among the young people filling streets, real questions remain about whether their protests will spur action from policymakers.

Thunberg and others have said they were inspired by students from Parkland High School who became activists after last year's deadly shooting at their school. But those efforts, along with a massive youth-led demonstration last year in favor of stronger gun laws, known as March for Our Lives, have not yet led to meaningful legislation.

Children hold placards as part of the climate strikes in Manila. ***Source:*** washingtonpost.com

One of Friday's first planned demonstrations — in Christchurch, New Zealand — had to be cut short when a heavily armed gunman attacked two mosques. The massacre of at least 49 people brought together two scourges that have been the ominous background to young people's lives worldwide: mass shootings and a warming planet.

Many young climate advocates in the United States have said they want to see the so-called Green New Deal — or pieces of it — embraced by lawmakers. But so far, Democrats have remained divided over the ambitious proposals, and many Republicans, including President Trump, have mocked them as absurdly expensive while also questioning the scientific consensus around man-made climate change.

Still, the teens have won the backing of many leading environmental groups, including Greenpeace, the Sunrise Movement and 350.org. This month, more than 250 scientists released a letter of support for the school strikes.

In Europe, where the climate strikes have been filling plazas in capital cities for months, leaders such as German Chancellor Angela Merkel have endorsed the movement.

But other politicians have mocked it. Christian Lindner, leader of a pro-business party in Germany, urged students to stay in school, saying that "politics is for professionals."

In Washington on Friday, the young people gathered on Capitol Hill had a message for the politicians inside: Get moving. Standing toward the back of the crowd, 16-year-old Jerome Nkugwa spoke about how the impacts of climate change are expected to grow more severe over time. He nodded toward the Capitol.

"Something worse is coming," Nkugwa said. "We came out to remind them to do something about it."

Source: https://www.washingtonpost.com/world/school-climate-strikes-draw-thousands-to-the-streets-in-cities-across-the-globe/2019/03/15/ad365672-402d-11e9-85ad-779ef05fd9d8_story.html?noredirect=on&utm_term=.5fa51ba2d085

This scary map shows how climate change will transform your city

February 2019 — The central contradiction of climate change is that it is at once the most epic problem that our species has ever faced yet it is largely invisible to the average human. From the comfort of your home, you may not realize how climate change is already affecting mental health, or ripping apart ecosystems, or how cities like Los Angeles are taking drastic measures to prepare for water shortages.

The challenge for scientists, then, is raising the alarm on something that's hard to conceptualize. But a new interactive map is perhaps one of the best visualizations yet of how climate change will transform America. Click on your city, and the map will pinpoint a modern analog city that matches what your climate may be in 2080. New York city will feel more like today's Jonesboro, Arkansas; the Bay Area more like LA; and LA more like the very tip of Baja California. If this doesn't put the dire threat of climate change into perspective for you, I'm not sure what will.

The data behind it isn't anything new, but the public-friendly *repackaging* of that data, known as climate-analog mapping, represents a shift in how science reaches the public. "The idea is to translate global forecasts into something that's less remote, less abstract, that's more psychologically local and relevant," says University of Maryland Center for Environmental Science ecologist Matt Fitzpatrick, lead author on a new paper in *Nature Communications* describing the system.

Fitzpatrick looked at 540 urban areas in North America using three primary datasets. One captured current climatic conditions (an average of the years between 1960 and 1990), the second contained projections of future climates, and the third provided historic climate variability from year to year taken from NOAA weather records. (Depending on the city, climate might be more "stable," or swing more wildly between years.) The researchers considered temperature and precipitation in particular, though of course these aren't the only two variables when modeling the climate—more on that in a bit.

If you click around the interactive map, you'll notice some trends under a scenario where emissions continue to rise for 60 years. "Many East Coast cities are going to become more like locations to the southwest, on average roughly 500 miles away," says Fitzpatrick. On the West Coast, cities look generally like places straight south of them. Portland, for instance, will in 2080 feel more like California's Central Valley, which is generally warmer and drier. Also, the map has an option (on its left side) that uses a different calculation to show what the shifts would look like if emissions peak around 2040 and begin to fall.

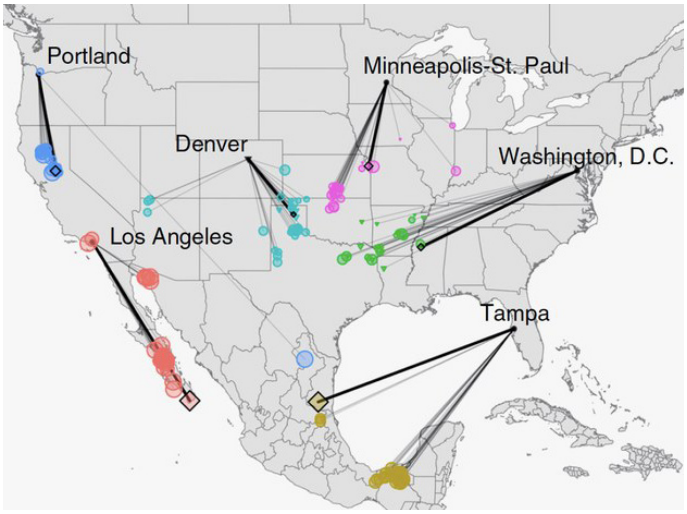

The implications are shocking, but also potentially useful. "Framing results in a digestible manner for the public sector, to inform policy, and for the scientific community, is notoriously difficult," says University of Wisconsin–Madison climate scientist Kevin Burke, who wasn't involved in the study. "One notable outcome of this work is the potential for cities and their analog pairs to transfer knowledge and coordinate climate adaptation strategies."

Take extreme heat, for example. That's a norm in a place like Phoenix, a city loaded with air conditioners. But in a place like San Francisco, air conditioning is a rarity. If San Francisco does indeed end up with a climate like LA's in 60 years, that's going to be a big public health problem. Extreme heat easily kills, as in Europe's deadly heat waves in 2017.

Another major consideration is water. Many urban areas will get drier, but others may see their total precipitation remain unchanged. However, the patterns of rainfall could change—to all fall in the winter, for instance. "So even though it's getting the same amount, that could have really large implications for places that aren't used to having an extended summer drought, or what have you," says Fitzpatrick.

San Francisco could stand to learn some water management techniques from its 2080 analog. Climate models predict that in the coming decades, LA will see fewer, yet more intense rainstorms. So to prepare, the city has begun an ambitious program to capture those huge dumps of water with a network of cisterns built into road medians. The rain capture program reduces its reliance on water piped into the city from afar.

The Bay Area, which has been historically blessed with more rainwater than its neighbor down south, hasn't been so forward-thinking. Rich communities have

thrown hissy fits when new water requirements meant their lawns would—gasp—turn brown. "Los Angeles is far ahead of the Bay Area in terms of having put in place incentives to move away from the more water-intensive outdoor landscaping that we still have even in the progressive Bay Area," says Michael Kiparsky, director of the Wheeler Water Institute at UC Berkeley, who wasn't involved with this new work.

Changes in rainfall would have serious implications for agriculture, of course. But something more subtle will also unfold: As the climate changes, so too will the makeup of local ecosystems. Pests like mosquitos, for example, could boom in your community. Certain plant species might not be able to handle the sudden shift and die out.

"Humans might adapt to some extent, and move, but animals and ecosystems won't be able to in that short time period," says Swiss Federal Institute of Technology climate scientist Reto Knutti, who wasn't involved in the study. "So we are pursuing a risky experiment with the Earth, with partly unknown consequences."

"That's actually my biggest worry," says Fitzpatrick. "It's not necessarily the direct changes in climate, it's these indirect impacts on natural and agricultural systems given the magnitude and rate of these changes."

More frightening still, some of the North American cities that Fitzpatrick explored will have no modern equivalent in 2080. That is, you can't compare them to a climate we see today. Which makes reacting to the threat all the more difficult—the Bay Area can anticipate feeling more like Los Angeles in 60 years and adapt accordingly, but if you don't have a good idea of what's coming, it's hard to mitigate against the threat.

To be clear, though, this climate analog technique simplifies things—for instance, the researchers left out complicating factors like the urban heat island effect, in which cities absorb more heat than surrounding rural areas. And this is average climate, not weather. So for instance, the recent cold snap on the East Coast was generated by warmer temperatures in the Atlantic.

"None of that's being captured by these analogs," says Andrew Jarvis, a scientist at CGIAR, an agricultural research institute. "So from a communication perspective, that's one of the dangers of it. It's overly simplifying." And necessarily so: Climate systems are monumentally complex, though bit by bit scientists are getting a better grasp on how our planet will transform in the time of climate change. A map alone can't communicate all of that knowledge.

Still, the idea with this new interactive map is to better visualize—both for regular citizens and policymakers—what has previously been presented as impenetrable datasets. "I hope more than anything it's an eye opener and that it starts more of these discussions so that more planning can take place," says Fitzpatrick.

Climate change is here, and it's already wreaking havoc. Consider this, then, a roadmap to help navigate the chaos.

Source: https://www.wired.com/story/this-scary-map-shows-how-climate-change-will-transform-your-city/

Not Trusting FEMA's Flood Maps, More Storm-Ravaged Cities Set Tougher Rules

A growing number of cities are looking beyond the usual 100-year floodplain and requiring more homes to be built higher for their own protection.

March 2019 — In flood-prone regions of the country, a growing number of cities have lost confidence in the ability of the federal government's flood maps to recognize the increasing risks that come with global warming.

From Houston to Baltimore to Cedar Falls, Iowa, and now Mexico Beach, Florida, local officials are going beyond the federal standards and have started to require homes in a much wider area—beyond the usual 100-year floodplain—to be built to higher flood-protection standards.

In Mexico Beach, the move was triggered in part by the Federal Emergency Management Agency's decision to reclassify dozens of properties that flooded last year in Hurricane Michael. The homes had been in the high-risk 100-year flood zone, where flood insurance generally is required, but FEMA moved them to the minimal-risk 500-year flood zone, where flood insurance is optional.

The city's goal is to have more homes and businesses higher and drier, so they're less likely to suffer flood damage when the next storm hits.

Hundreds of communities and as many as 22 states already require new construction be elevated higher than federal requirements in the high-risk 100-year floodplain, which is based on a 1 percent chance of flooding in any given year. Now, a small but growing number of cities and counties are also extending the additional building-height standards to the wider 500-year floodplain.

Officially, the 500-year floodplain means a 0.2 percent annual chance of flooding, but climate change may be loading the dice for higher risks.

"We now are seeing this trend start because people are getting these extreme events," said Larry A. Larson, a professional engineer and senior policy advisor for the national Association of State Floodplain Managers.

"We have people outside the high-risk area getting flooded," he said. "If we regulate to the 500-year (risk) we are more apt to get closer to what we call the 100-year but really now is more than that."

The threat will only get worse as communities pack more development into low-lying areas and as global warming fuels more extreme weather, said Shana Udvardy, a climate resilience analyst with the Union of Concerned Scientists.

In the newest National Climate Assessment, published last fall, U.S. government scientists warned that global warming was intensifying and increasing the frequency of extreme rainstorms that cause devastating flooding. Hurricane rainfall and intensity are also likely to increase, as are the frequency and severity of "atmospheric rivers" of rain on the West Coast, like the event that drenched California last month, triggering flash floods and mudslides. Sea-level rise also makes storm surges more dangerous.

Flooding spread through block after block of Houston as the remnants of Hurricane Harvey dropped 50 inches of rain in some areas in 2017. Homes on properties that had been built up to raise their elevation were more likely to escape interior damage. *Source:* https://insideclimate-news.org/

But FEMA hasn't taken climate change into account when creating flooding maps.

FEMA Plans Risk-Rating Changes, but Mexico Beach Sees Bigger Problem

Floodplains are mapped by FEMA to determine which properties are likely to be inundated under different risk scenarios.

People with federally backed or regulated mortgages on buildings in the 100-year floodplain are required to buy insurance through the National Flood Insurance Program, which has fallen under extreme stress from repeated, major national flooding disasters and is billions of dollars in debt.

On Monday, FEMA announced it was rolling out a new risk-rating system to determine insurance premiums that will use more risk factors to calculate insurance costs for each property. But it still only requires flood insurance for homes in the 100-year floodplain.

Some communities, like Mexico Beach, join a lot of experts in saying those FEMA flood maps are misleading

and downplay overall flood risk.

In Mexico Beach, new draft maps reclassify about 40 properties into the 500-year, minimal-risk zone that were severely damaged by Hurricane Michael's surging waters. Twenty of those buildings were completely destroyed, said Katie McDowell Peek, a coastal geologist with Western Carolina University's Program for the Study of Developed Shorelines, which carried out the analysis. Some were once beachfront homes.

"We were shocked they were removed" from the high-risk zone, Peek said, adding that she and her colleagues have seen the same thing happen with other FEMA remapping, including in Dare County, North Carolina.

The FEMA maps are based on a scientific analysis of ground elevations and contours, said Jerrick Saquibal, hydrology and engineering chief with the Northwest Florida Water Management District, which is working with FEMA to develop flood maps for Mexico Beach and other nearby communities.

They are drawn for insurance purposes and are not meant to convey an overall flood risk, especially from a record storm like Michael, he added. Flood-prone communities like Mexico Beach are encouraged to adopt their own, more stringent regulations, in either flood zone, he said.

Mexico Beach Mayor Al Cathey said he didn't understand the new draft FEMA maps, which, when adopted, will mean homes that are rebuilt on those properties will no longer be required to buy flood insurance.

Without the new city ordinance, there also would have been no extra elevation requirements, he said. But now, he said, new construction must be elevated at least a foot and a half higher than FEMA's base-level flood predictions in both the 100-year and 500-year floodplains, which encompass most of the town, which had a population of about 1,200 before Michael.

"As the local government, it is our responsibility to protect our citizens," said Cathey, adding that the decision was made as a direct result of Michael, with its approximately 19-foot storm surge that swept dozens of homes off their foundations and damaged even more.

"I felt we needed to show FEMA that we are going a step beyond what they say is necessary."

Coastal and River Cities Setting Higher Standards

Mexico Beach's new floodplain regulations are part of a shift, floodplain experts said. Houston made similar changes in the aftermath of catastrophic flooding from Hurricane Harvey in 2017. So did Baltimore after multiple floods, including Hurricane Isabel, which made more than 570 homes and 15 businesses uninhabitable because of flooding.

"The (FEMA) maps are based on historical data and in many cases are old and outdated, so communities are seeing flood impacts that are going well beyond the areas that FEMA regulates," said attorney Jessica Grannis, the adaptation program director at the Georgetown Climate Center in Washington, D.C.

A photo of Mexico Beach looking east across the canal shows several of the properties where homes were destroyed that FEMA's draft map moves from the high-risk 100-year floodplain to the lower-risk 500-year floodplain. ***Source:*** https://insideclimatenews.org/

The Georgetown program in January issued a report on how Maryland's eastern shore could adapt to increasing concerns about flooding and sea level rise. Regulating the 500-year-floodplain was among the recommendations of the report, which cited rules in Cedar Falls and Baltimore as examples.

Cedar Falls, which has a 1-foot elevation requirement above base flood levels, according to FEMA, is experiencing flooding again this week after a major storm in the region.

Baltimore requires new construction or substantial reconstruction to be elevated 2 feet above a base flood level, providing an extra margin of safety. The city has a long history of flooding. In 2003, its coastal neighborhoods were inundated by tidal flooding from Hurricane Isabel, causing severe damage, said Victor Ukpolo, the city's floodplain manager. In 2014, the city experienced more extreme flooding.

"The severity of these flood events, and anticipating more frequent and severe climate threats, led to adopting the higher standard," he said.

In Charlotte and Mecklenburg County, North Carolina, local authorities map what they call a future conditions floodplain that's roughly equivalent to a FEMA 500-year floodplain, with 1- to 2-foot building elevation requirements, said Timothy J. Trautman, the area's stormwater services manager. It has taken anticipated land-use changes into account for 15 years, he said.

Those efforts may have spared thousands of homes from flooding during last year's Hurricane Florence, which hammered North Carolina, he said.

After Harvey, Houston Strengthens Building Rules

A FEMA spokeswoman said the agency doesn't track how many of the 22,000 American communities that participate in the National Flood Insurance Program are voluntarily adding flood protection requirements in the 500-year floodplain.

But in April last year, FEMA praised the Houston City Council for "ensuring new construction will meet a higher standard for flood preparedness" by requiring 2 additional feet between expected flood levels and new development in both the 100- and 500-year floodplains.

The remnants of Hurricane Harvey dumped roughly 50 inches of rain on parts of Houston over four days in August 2017, flooding more than 150,000 homes in that city alone, according to a city study. That study concluded that if all of Houston's homes had been compliant with the city's new rules, 84 percent of the city's homes that flooded during Harvey would have been spared.

That study estimated that the new requirements would add $11,000 to $32,000 to the cost of newly constructed homes, while the savings from avoided flooding costs could range from $50,000 to many hundreds of thousands of dollars—not including the value of avoided risk to first responders, emotional trauma and health impacts.

Harris County, surrounding Houston, passed similar floodplain requirements following Harvey.

"It's revolutionary in the sense that we've never really had regulations so tied to the floodplain at that level of protection," said Iris Gonzalez, the coalition director at Coalition for Environment, Equity and Resilience in Houston. In the aftermath of Harvey, Houston has a "bigger appetite" for "making sure we are building a Houston that can withstand these kinds of weather events that are more frequent."

But she also cautioned that adding more expensive building requirements can hurt low-income and minority families, forcing them out of affordable neighborhoods. "It comes down to designing programs with that in mind," she said, such as directing financial help to some of those neighborhoods.

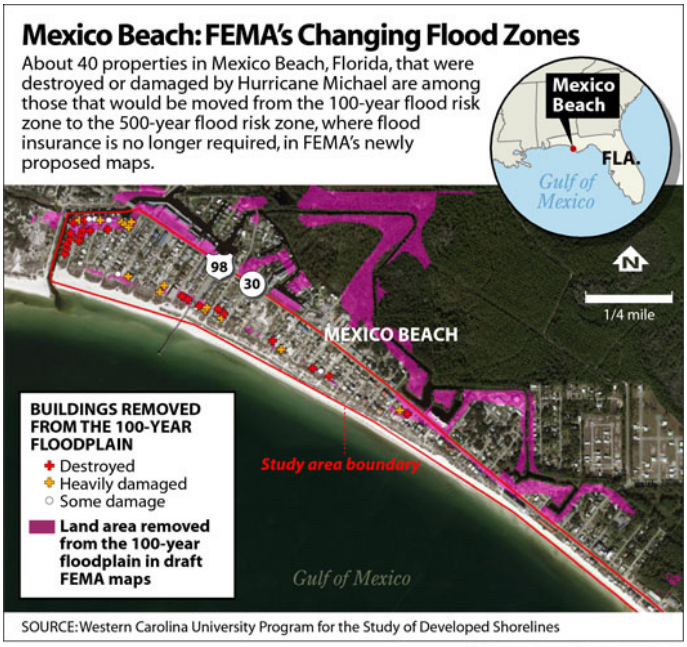

PAUL HORN / InsideClimate News

We Want People to Build Their Houses Safely

In Dare County, North Carolina, authorities are preparing to regulate building heights in the 500-year-floodplain, said Donna Creef, the county's planning director. The county includes 110 miles of fragile, sand-shifting barrier islands known as the Outer Banks.

As in Mexico Beach, newly drawn draft FEMA maps are putting properties that have been in the high-risk 100-year floodplain into the 500-year floodplain, which would exempt them from insurance requirements and local elevation requirements.

Yet Creef said these properties, which are vulnerable to storm surges from hurricanes, have flooded and will flood again. So the plan is to propose a higher standard across a larger area to include the 500-year floodplain, she said.

"We want people to build their houses safely," and to have insurance, Creef said. *Source:* https://insideclimatenews.org/news/19032019/fema-flood-maps-risk-zones-cities-climate-change-mexico-beach-houston-outer-banks

This story was co-published with The Weather Channel as part of Collateral, a series on climate, data and science.

As China Cuts Air Pollution, An Unseen Killer Emerges

Efforts to cut smog-causing PM 2.5 are leading to rises in ground-level ozone, a chemical harmful to health.

February 2019 — China's smog-choked air is already a public health crisis, with around 1 million deaths attributable to air pollution every year, according to the World Health Organization. But as the government works to dissipate the gray haze blanketing the country's cities, an invisible killer is rearing its ugly head: ozone. It has the country's public health experts worried.

"China should pay more attention to ozone control," says Zhang Junfeng, a professor of global and environmental health at the Regional Ozone Sino-US Collaborative Research Center at Duke Kunshan University, China's first research institute for ozone pollution control, established in 2016. "Once ozone gets into the human body, it causes considerable damage to the immune system and aggravates existing cardiovascular and respiratory problems."

Ozone is best known as the layer of gas in the earth's atmosphere that protects humans from harmful ultraviolet rays, exposure to which can cause cancer and other health issues. Indeed, China came under global criticism for failing to control domestic emissions of chlorofluorocarbons — or CFCs — chemicals that deplete global ozone levels and increase health risks.

However, less well-known is the fact that too much ozone at the ground level is also a public-health threat. Air with high ozone concentrations can damage cells in the lungs and other organs. In China, an estimated 316,000 adults died in 2010 from respiratory illnesses caused or aggravated by ozone pollution, according to a study into long-term ozone exposure published in 2017 by the journal *Environmental Health Perspectives*. In addition, roughly one-quarter of the world's ozone-attributable respiratory deaths occur in China.

Ozone accumulates when airborne nitrogen oxides — mostly produced by coal burning and vehicle emissions — react with volatile organic compounds (VOCs), organic chemicals that evaporate easily, even at room temperature. Although the Chinese government's air-pollution control policies have been reducing atmospheric nitrogen oxides since 2012, they are less efficient at controlling VOCs, leading to a buildup of ground-level ozone.

Zhang says that China's ozone problem is aggravated by the fact that public discussion on air pollution focuses heavily on so-called atmospheric particulates — microscopic solid or liquid matter suspended in the air that contributes to visible smog in the cities. Particulates with diameters of 2.5 and 10 micrometers or less — known respectively as PM 2.5 or PM 10 — are known to be deadly, potentially causing cancer, heart attacks, and respiratory disease. Consequently, the Chinese government has implemented a series of measures that aim to reduce levels of atmospheric PM 2.5 and above, while efforts to cut ground-level ozone levels have stalled.

"The public is well-informed about how PM 2.5 causes heavy air pollution, and the authorities have put a lot of effort in recent years into bringing PM 2.5 and PM 10 under control," says Zhang. "It's obvious that these pollutants have fallen. But ozone pollution … doesn't receive the same amount of attention, either from the public or from the government, because it's far less visible in the first place."

Accordingly, China's air quality policies prioritize PM 2.5 reductions ahead of ones for ozone, says Hao Jiming, a professor of environmental engineering at Beijing's Tsinghua University. "Currently, China's standard for safe levels of atmospheric PM 2.5 is 3.5 times higher than WHO's air quality guidelines," Hao explains — a target that certain parts of the country fail to meet, despite the additional leeway. Meanwhile, national standards for ground-level ozone are only 1.6 times higher than WHO and are breached less dramatically, further focus-

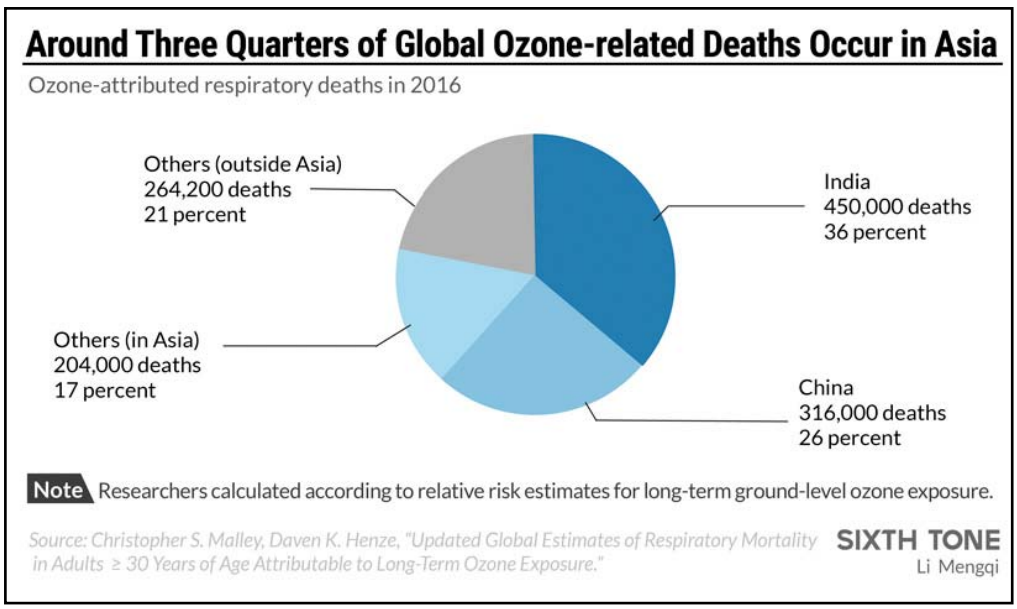

ing attention on PM 2.5, Hao adds.

Last month, scientists from Harvard University and Nanjing University of Information Science & Technology published a paper showing how China's war on PM 2.5 has unexpectedly driven up ozone pollution. Normally, the presence of PM 2.5 in the air disrupts the chemical reactions between the free radicals that produce ozone. When PM 2.5 levels fall, these reactions become more likely, and so more ozone is produced. The negative effects on ozone pollution from drastically decreasing PM 2.5 are particularly noticeable in regions like the North China Plain, a former industrial region that has been a key target of pollution reduction in recent years.

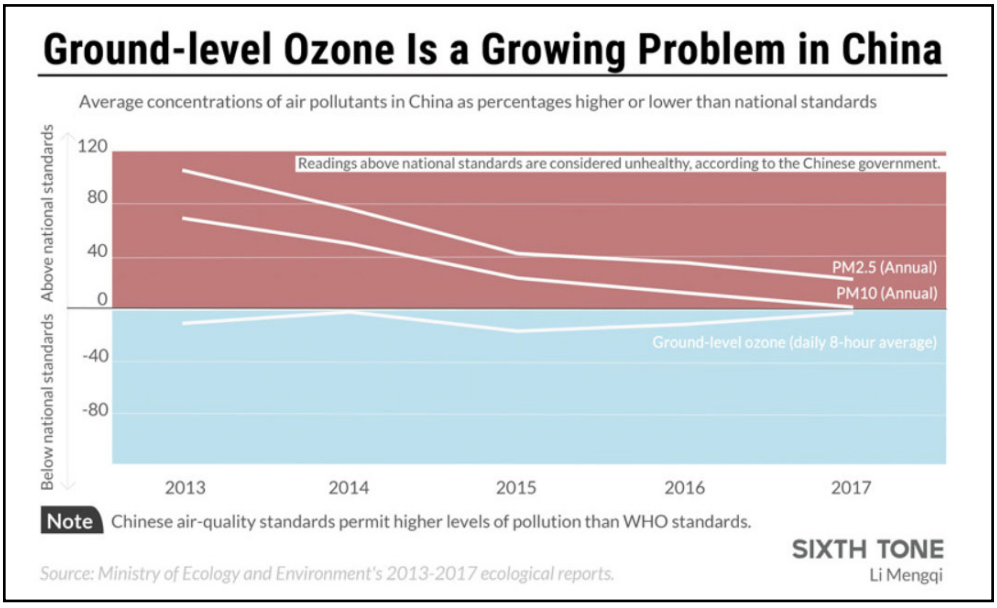

In a January interview, one of the paper's co-authors, Daniel Jacob, drew attention to the uniqueness of China's ozone problem. "We haven't observed this happening anywhere else, because no other country has moved this quickly to reduce [PM 2.5] emissions," Jacob said. "It took China four years to do what took 30 years in the U.S."

In their paper, Jacob and his colleagues recommended that China establish effective measures to cut ozone pollution by controlling the release of its precursors — nitrogen oxides and VOCs. But Zhang, the professor at Duke Kunshan, says cutting ozone pollution may be even more challenging than controlling particulates — partly because it's difficult to identify the origin of ozone pollution in the first place.

"Ozone trends are different in different parts of China. Understanding which of the precursors is driving ozone formation in a city or a region is the first step toward ozone control," Zhang says, adding that research into ozone pollution is dramatically lacking compared with research into PM 2.5. "In many regions, it's still unclear what's really causing ozone levels to increase," he adds.

Without robust ozone control measures, many Chinese people will likely face greater health risks in the future. Across the country, climate change and global warming are prolonging and intensifying periods of warm weather in which ozone becomes more highly concentrated. At the same time, China's population is growing older and more vulnerable to the adverse health effects of ozone pollution.

"If climate change continues at the current rate, ozone pollution will cause higher mortality rates in the future," says Chen Kai, a postdoctoral fellow at the Alexander von Humboldt Foundation in Germany. Chen's research, in collaboration with Columbia University, shows that China's mortality rates linked to short-term ozone exposure could quadruple within 40 years, due largely to global warming and the country's aging population.

China's latest three-year plan to curb air pollution, released in July 2018, does make certain provisions for ozone control, such as compelling manufacturers to repair and replace VOC-emitting installations and applying legal upper limits on VOC concentration in paints, inks, and adhesives. And in the Yangtze River Delta, experts are already teaming up with government authorities to combine controlling PM 2.5 with protecting against excessive ozone by curbing industrial emissions, vehicle exhaust fumes, and coal burning.

"If China does not pay enough attention to ozone pollution now, it'll be tough to tackle it in the future," Zhang says. *Source:* https://www.sixthtone.com/news/1003590/as-china-cuts-air-pollution%2C-an-unseen-killer-emerges

A 100-meter-tall air purifier in Xi'an City, Shaanxi province, Jan. 17, 2018. Source: www.sixthtone.com


Estimating gross primary productivity with high spatial resolution satellite imagery over the Minneapolis-Saint Paul, USA metropolitan region

By David L. Miller (dlm@ucsb.edu) **and Joseph P. McFadden** (mcfadden@ucsb.edu)
Department of Geography, University of California, Santa Barbara, USA

This article summarizes a recently published paper and related work: Miller, D.L., Roberts, D.A., Clarke, K.C., Lin, Y., Menzer, O., Peters, E.B., McFadden, J.P., 2018. Gross primary productivity of a large metropolitan region in midsummer using high spatial resolution satellite imagery. Urban Ecosystems 21, 831–850. https://doi.org/10.1007/s11252-018-0769-3

Introduction

The sum of photosynthesis at the ecosystem scale is known as gross primary productivity (GPP), which quantifies the initial input of carbon to ecosystems and is an important metric of ecosystem function. While there are well-established satellite remote sensing-driven models of GPP for natural ecosystems, urban areas are not usually included in such models (e.g., Running and Zhao, 2015), largely due to the small percentage of the global land area covered by cities relative to the major natural biomes and due to the fine-scale spatial heterogeneity of urban areas.

In general, urban development reduces primary production in densely vegetated regions (Imhoff et al., 2004), but urbanization can increase primary production in some areas previously covered by agriculture (Zhao et al., 2007) or deserts (Buyantuyev and Wu, 2009). Urban vegetation can provide a multitude of ecosystem services, such as local cooling (Oke, 1989) and absorption of airborne pollutants (Nowak et al., 2006), and can affect carbon budgets both directly and indirectly. There is a need for mapping GPP within urban areas because it is relatively unknown how GPP varies among vegetation and land-use types in cities.

One of the most established methods to calculate GPP from remote sensing is the light use efficiency approach, first proposed by Monteith (1972), which assumes that vegetation takes up carbon at a rate relative to incoming solar radiation such that:

$$GPP = FPAR \times PAR \times LUE \quad [1]$$

GPP is the mass of carbon taken up per unit time (g C m^{-2} d^{-1}), PAR is the incident photosynthetically active radiation from the sun per unit time (MJ m^{-2} d^{-1}), FPAR is the unitless fraction of PAR absorbed by vegetation, and LUE is the conversion rate from absorbed PAR to plant carbon uptake (g C MJ^{-1}) (Hilker et al., 2008).

Due to the fine scale spatial heterogeneity of urban areas, there are two major challenges in applying production efficiency models of GPP in cities. First, it is difficult to identify and map individual urban vegetation types, which have different LUE parameters. Second, it is difficult to obtain accurate estimates of FPAR due to the mixing of vegetated and non-vegetated surfaces in the relatively large pixels of many satellite remote sensing systems. In addition, due to lack of urban vegetation measurements, many studies of urban GPP have used non-urban LUE values from natural ecosystems (e.g., Milesi et al., 2003; Zhao et al., 2007); few studies have relied on locally-parameterized LUE values specific to urban vegetation types (e.g., Wu and Bauer, 2012).

In this study, we used high spatial resolution WorldView-2 satellite imagery (2 m pixels) over Minneapolis-Saint Paul, Minnesota, USA. This imagery allowed us to make a detailed classification of urban vegetation types and to assign different LUE values to each, and it allowed us to more accurately estimate FPAR for vegetated areas because mixed pixels were reduced. We then used in situ carbon flux measurements to derive GPP and the WorldView-2 imagery to retrieve FPAR, producing empirical LUE values for each vegetation type in the study area (deciduous broadleaf trees, evergreen needleleaf trees, turf grass, and golf course grass). We used our parameterized LUE values to estimate GPP across the WorldView-2 imagery, and compared our mapped estimates to GPP observations from a tall tower (KUOM).

Our research questions were: (1) what is the magnitude and variability of GPP within the dominant urban vegetation types, (2) what determines the magnitude and variability of GPP within the major urban land-use types, and (3) how does GPP for urban vegetation compare to natural vegetation?

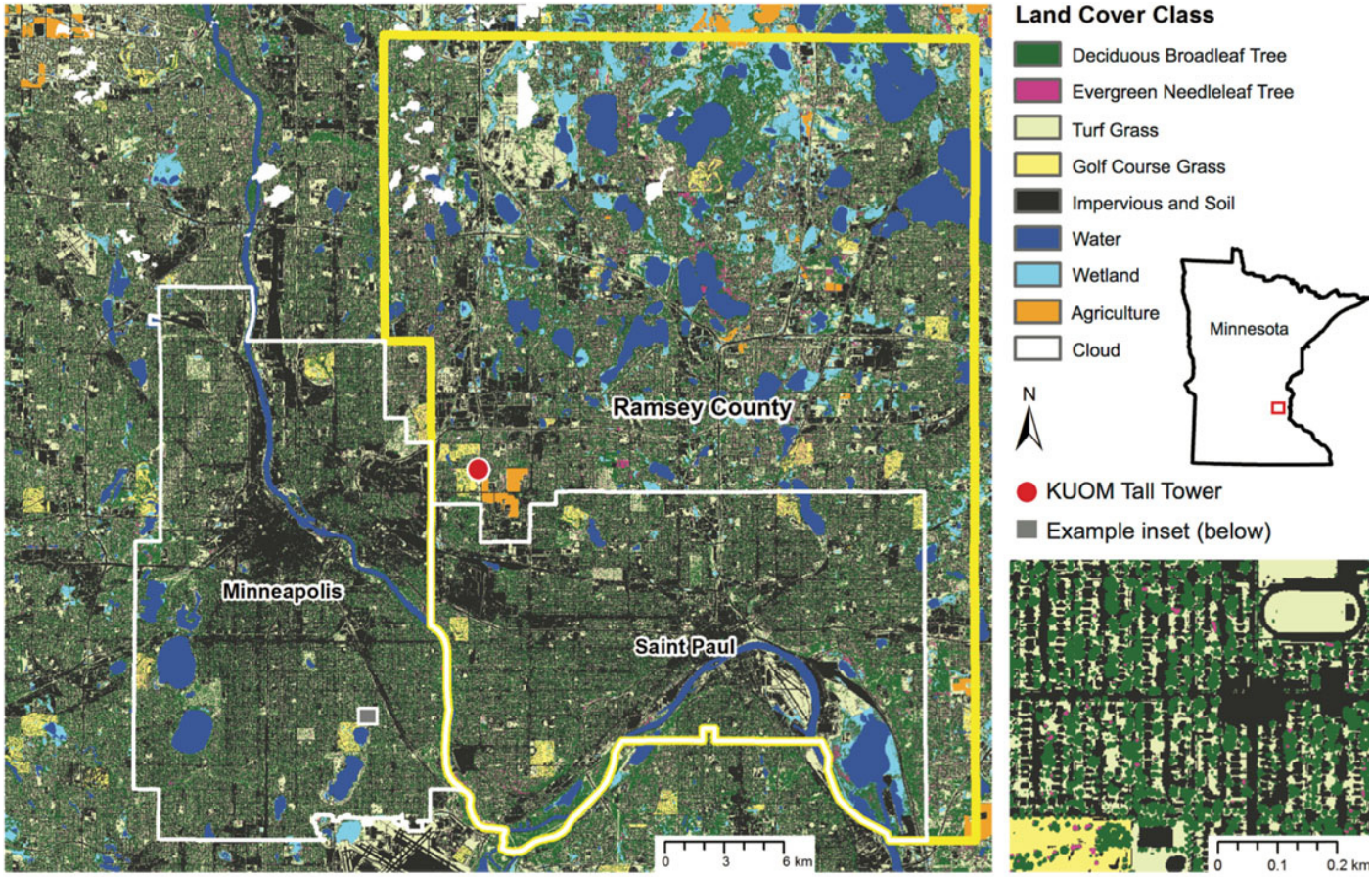

Figure 1. Land cover classification for the full study extent (32 x 28 km) (left) with the KUOM flux tower location indicated by a red circle, the Minneapolis and Saint Paul boundaries by the white lines, and the Ramsey County boundary by the yellow lines. Inset (lower right) location indicated by gray box. Location of the study area in Minnesota indicated by red box in state outline (right).

Methods

Our study site was a large part (894 km^2) of the Minneapolis-Saint Paul, Minnesota (44° 59′ N, 93° 11′ W) metropolitan region. The region has a humid continental climate (Köppen Dfa) with year-round precipitation and warm summers and cold winters. Within this region the KUOM tall tower flux site provided a rare opportunity for scaling up urban GPP because CO_2 fluxes over multiple years had been measured separately for each of the dominant urban vegetation types, including deciduous broadleaf trees, evergreen needleleaf trees, and turf grass (Peters and McFadden, 2012). We used eddy covariance measurements acquired at 40 m height on the KUOM tower to compare with our mapped GPP (Menzer and McFadden, 2017).

The WorldView-2 imagery was acquired on July 17 and July 28, 2010 at 2 m spatial resolution. It was orthorectified and coregistered to a 1 m spatial resolution lidar digital surface model and atmospherically corrected with the FLAASH module in ENVI 5.1. We scaled linear offsets in the Normalized Difference Vegetation Index (NDVI; NIR – red / NIR + red) using sampled areas from the overlapping region of the images, and the images were mosaicked. We classified urban vegetation using a hierarchical approach including a maximum likelihood classifier, lidar-derived height thresholding, leaf-off aerial orthophotography, and GIS data available from the Metropolitan Council and other sources.

FPAR was derived from WorldView-2 NDVI using a linear relationship from Sims et al. (2006):

$$FPAR = 1.24 \times NDVI - 0.168 \quad [2]$$

This relationship had been derived from NDVI from the MODIS satellite sensor, and we scaled our WorldView-2 NDVI to MODIS NDVI using spectrally resampled bands from a NASA Airborne Visible Infrared Imaging Spectrometer (AVIRIS) image of a nearby site acquired on July 29, 2009. We used the resulting NDVI to calculate FPAR.

To derive an empirical LUE estimate for each vegetation type, we used in situ observations of tree and turf grass GPP and PAR in a first-ring suburban neighborhood in the center of our study area. For trees, we used GPP estimates based on sap flow and leaf-level gas exchange measurements from on seven genera representing evergreen needleleaf and deciduous broadleaf tree

Table 1: Comparisons between our empirical LUE estimates and estimates for scaled MODIS GPP (MOD17; Running and Zhao, 2015) LUE by vegetation class. LUE estimates are g C MJ^{-1} PAR.

This Study		Estimated MODIS GPP	
Vegetation Class	LUE	Vegetation Class	LUE (VPD = 2.018 kPa)
Deciduous Broadleaf Tree	0.24	Deciduous Needleleaf Forest	0.19
Evergreen Needleleaf Tree	0.56	Deciduous Broadleaf Forest	0.00
		Evergreen Needleleaf Forest	0.63
		Evergreen Broadleaf Forest	0.60
		Mixed Forest	0.23
		Closed Shrubland	0.85
		Open Shrubland	0.56
		Woody Savanna	0.57
Turf Grass	0.66	Savanna	0.53
Golf Course Grass	1.14	Grassland	0.61
		Cropland	0.65

plant functional types (Peters and McFadden, 2012). For turf grass, we used GPP estimates from eddy covariance CO_2 flux measurements acquired at a 1.5 ha turf grass field. For golf course grass, we used modeled estimates of turf grass GPP from Peters and McFadden (2012) from the turf grass site when water was not limiting growth in the spring and fall. We also made an independent assessment of our mapped GPP estimates using eddy covariance CO_2 flux measurements from a height of 40 m on the KUOM tall tower near the turf grass and tree sites. PAR was derived from downwelling shortwave radiometer measurements at all sites.

From the in situ measurements, we generated characteristic mean diurnal cycles of midsummer daily GPP and PAR for the plant functional types of interest and the tall tower footprint. These were estimated based on half-hourly data from a 4-week interval centered on the July date of acquisition for the WorldView-2 imagery. Each half-hourly time point was averaged, and these averages during daylight were summed to produce composite diurnal estimates of GPP (g C m^{-2} d^{-1}) and PAR (MJ m^{-2} d^{-1}). The FPAR for each target vegetation class was estimated from manually drawn polygons on the WorldView-2 derived FPAR map. The empirical LUE estimates were calculated using the site polygons' FPAR and the vegetation types' 4-week GPP and PAR values.

We generated our GPP map with the LUEs based on vegetation type in the classification, the WorldView-2 FPAR raster, and the 4-week PAR from the tall tower observations (12.09 MJ m^{-2} d^{-1}). The mapped GPP was compared to the 4-week mean GPP estimates for the 40 m tall tower by extracting the GPP values within the composite 80% flux source area of the KUOM tower's 40-m level.

Results and Discussion

The land cover classification had an overall accuracy of 80% (kappa = 0.74) for built-up and vegetated land cover classes (Figure 1). In terms of FPAR, deciduous broadleaf trees, evergreen needleleaf trees, and golf course grass all had similarly high values (mean ~0.86 ±0.09 SD), while turf grass FPAR was lower and was more variable (0.76 ± 0.13).

LUE was lowest for deciduous broadleaf trees and highest for golf course grass, with evergreen needleleaf trees and turf grass in between (Table 1). We found our values were comparable to some, but not all, estimates of the MODIS GPP product (MOD17; Running and Zhao, 2015) using measured vapor pressure deficits at our sites. For example, our deciduous broadleaf tree LUE was similar to the MODIS GPP mixed forest LUE, and higher than the MODIS GPP deciduous broadleaf tree LUE. Our grass LUE values bracketed the range of published LUE values for natural vegetation, with golf course grass having higher LUE and turf grass having lower LUE compared to natural grasslands. Our evergreen needleleaf and deciduous broadleaf tree LUE values were lower than most published values for forests.

Overall, golf course grass had the highest mean mapped GPP (11.77 g C m^{-2} d^{-1}), followed by turf grass (6.05 g C m^{-2} d^{-1}), evergreen needleleaf trees (5.81 g C m^{-2} d^{-1}), and deciduous broadleaf trees (2.52 g C m^{-2} d^{-1}) (Figure 2, Figure 3). Mapped turf grass GPP had a coefficient of variation (CV = SD/mean) that was nearly twice as large as the other vegetation classes (0.18 vs. ~0.10), which is likely attributable to greater variability in the effects of maintenance, including fertilization and irrigation. The tall tower GPP estimate was 8.01 g C m^{-2} d^{-1} for the 4-week

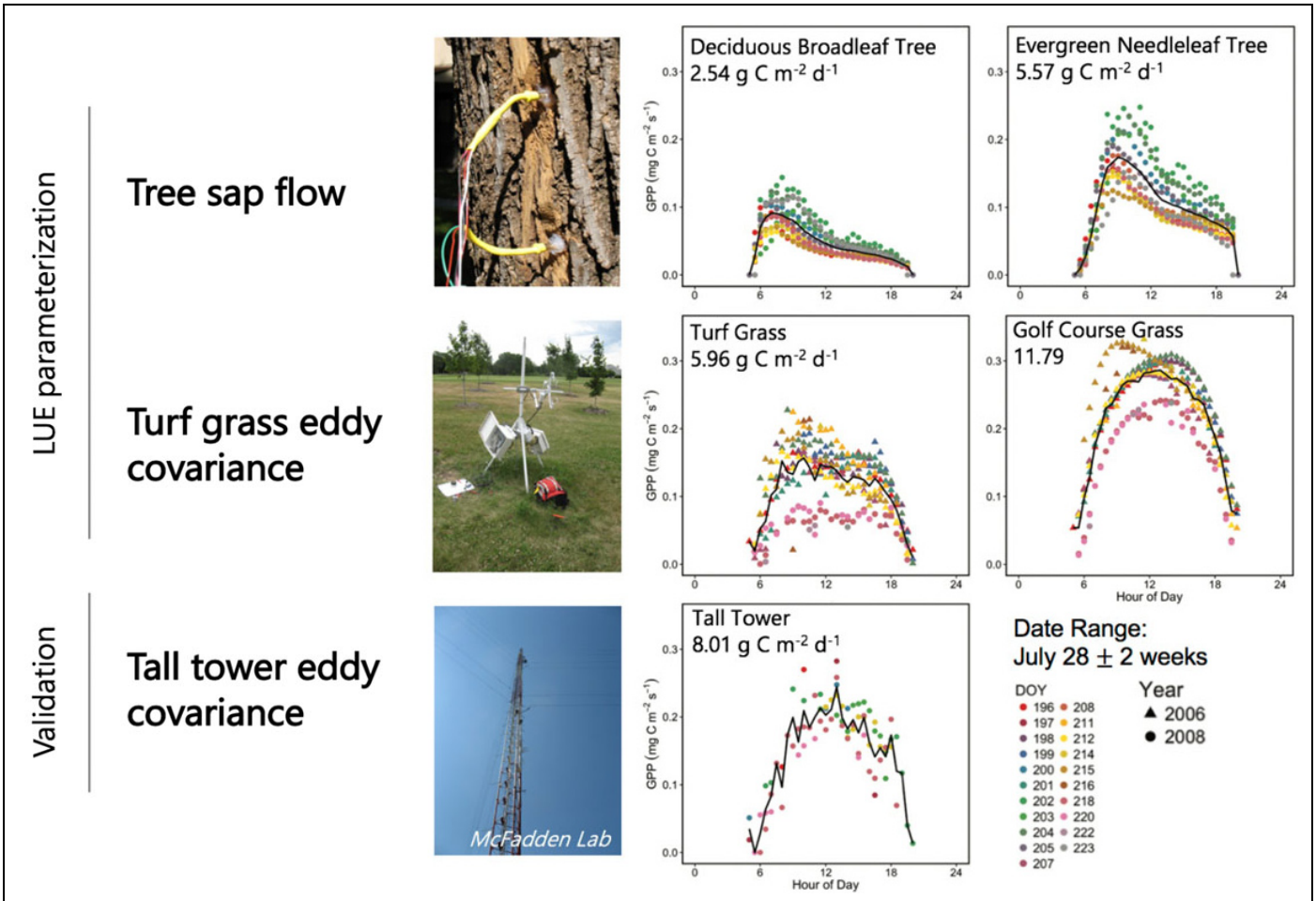

Figure 2. In situ flux observations (and related photos) used to calculate mean daily sums of GPP and PAR during 4-week interval centered on the WorldView-2 observation date. Mean values at half-hourly intervals are black lines, colors are day of year (DOY), triangles represent observations from 2006 and circles from 2008. Note that golf course grass GPP data were modeled based on turf grass eddy covariance measurements under peak growing conditions in 2006 and 2008. All data are during daylight (PAR > 0.45 W m^{-2}).

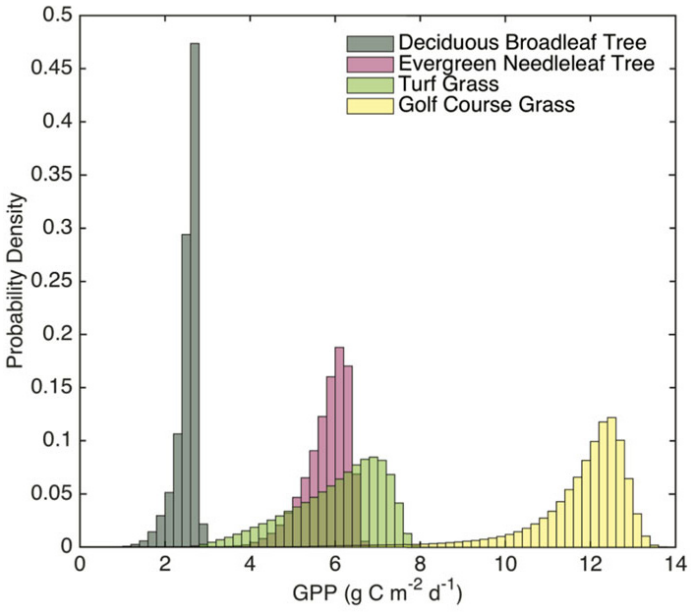

Figure 3. Normalized histogram of GPP (g C m^{-2} d^{-1}) for each vegetation cover type across the total metropolitan study area.

period, and the mapped GPP within the tall tower's 80% flux source area was 7.10 g C m^{-2} d^{-1}. The 11.4% difference was reasonable given the inherent variability in our GPP estimate and the uncertainties of eddy covariance flux observations and flux footprint modeling.

When averaged across the total urban land area (i.e., including built-up impervious surfaces and soil) the mean GPP was 2.64 g C m^{-2} d^{-1}, but when averaged over just the vegetated areas of the city GPP was 4.45 g C m^{-2} d^{-1} (Figure 4). The urban GPP per unit vegetated area fell at the low end of range that has been reported for natural vegetation of 5 to 14 g C m^{-2} d^{-1} in mixed forests, deciduous broadleaf forests, and grasslands in similar climate zones (Yuan et al., 2007). This may be due to differences in plant growth habit, environmental stresses, and vegetation composition in urban areas. In terms of overall GPP contribution, turf grass contributed 59.7% of the total urban GPP, while deciduous broadleaf trees were 27.8%, evergreen needleleaf trees were 6.3%, and golf course grass was 6.3%.

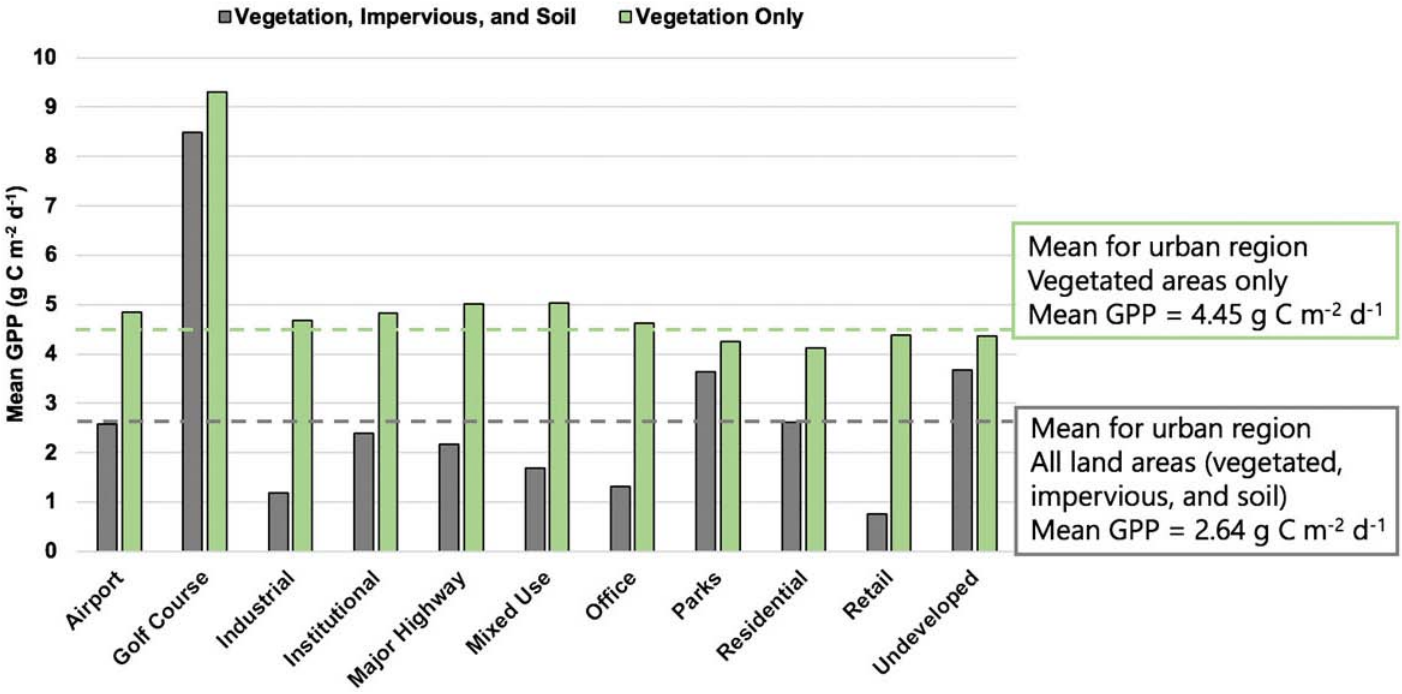

Figure 4. Mean GPP by land-use type. Gray bars include vegetation, impervious, and soil surfaces in their mean calculation, while green bars are for vegetated areas only. Dashed lines are mean values across the total study area for comparison.

When expressed per unit of total urban land area, we found large differences in mean GPP among land-use types, but when compared per unit vegetated area, the mean land-use GPP values varied within a relatively narrow range (Figure 4). The overall differences of GPP in different land-use types were mostly attributable to their percent vegetation cover. The mean GPP values of land-use types showed a strong linear relationship ($y = 0.04x + 0.21$, $R^2 = 0.98$, $p < 0.001$) with percent vegetation cover, not including golf courses (figure not shown). However, vegetation composition and GPP rates were important in determining the make-up of GPP contributions across land-use classes. In general, turf grass was dominant in determining GPP due to its large coverage and relatively high GPP, suggesting that the GPP of most land-use types would be highly sensitive to changes in turf grass cover or maintenance. The effects of trees were most important in the most tree-covered classes: park, recreational or preserve; undeveloped; and residential.

It is important to note that, because GPP is only the initial input of carbon to ecosystems, high rates of GPP do not imply high rates of carbon stored. GPP is counterbalanced by plant respiration, leaving behind net primary production (NPP). Peters and McFadden (2012) found that while the deciduous broadleaf and evergreen needleleaf tree species at our site were consistent net carbon sinks, our turf grass study site varied between a small net sink or a net source of carbon depending on the year (Hiller et al., 2011). Previous work has shown approximately half of forest GPP goes into NPP broadly speaking (DeLucia et al., 2007), but there is considerable variability due to many factors including stand age and local temperature reduction (Peters and McFadden, 2010). While mapping NPP was beyond the scope of this study, net carbon uptake over time in our study area is likely driven by trees rather than turf grass.

Conclusions

We analyzed variations in GPP across the Minneapolis-Saint Paul, USA metropolitan region. This was one of the first studies to report LUE values specific to urban vegetation and to quantify the spatial variability of GPP within individual vegetation types. We found that, while turf grass and deciduous broadleaf trees had similar percent cover in the study region, the lower LUE of deciduous broadleaf trees resulted in a lower contribution to overall GPP compared to turf grass. However, GPP was much more variable in turf grass than in the other vegetation types, likely due to management practices. While the overall metropolitan GPP was influenced by turf grass condition in our study area, the relatively high rates of turf grass GPP do not imply high rates of carbon storage because of respiratory carbon losses. Averaged over the total urban land area, urban GPP was lower than natural vegetation GPP mainly due to the reduced fractional cover of vegetation in urban areas. In contrast, the mean GPP within only the vegetated areas of the city fell at the low end of ranges reported for natural forests and grasslands in similar climate zones. The high spatial resolution imagery from WorldView-2 allowed us to separately parameterize vegetation types in our mapped GPP, and to compare both across and within vegetation type, land-use type, and cities. It is likely that fine spatial estimation of key variables used in quantifying ecosystem services and carbon accounting, such as GPP in this study, can be

valuable in targeting urban development approaches and greenspace management.

Ongoing related work

In our lab group, we are continuing to build off these results in two new directions. First, Olaf Menzer is using the WorldView-2 land cover classification described here to perform flux source area analyses of the KUOM tall tower data set. Based on a time series in which he has partitioned the net biogenic CO_2 flux from the total urban net flux (Menzer et al., 2017), he is using our high resolution vegetation map to attribute the net biogenic CO_2 fluxes to different plant functional types. Second, Sarah Beckingham is estimating total aboveground biomass (trees plus turf grass) at the level of individual residential parcels using NDVI, lidar, and GIS data across two counties (~1600 km^2) of the Minneapolis-Saint Paul metropolitan area. This project focuses on households that participated in a survey of carbon, nitrogen, and phosphorus fluxes (Twin Cities Household Ecosystem Project, Fissore et al., 2011). The remote sensing data are being used to develop models based on a large set of households at which plant biomass and annual carbon exchange were measured in the field by urban forest inventory and allometric models (UFORE; Nowak et al., 2008), and turf grass lawn measurements.

Acknowledgements

A grant from the NASA Earth Science Division (NNG-04GN80G) funded the field measurements at KUOM as part of the North American Carbon Program (NACP), and grant from the NSF Dynamics of Coupled Natural and Human Systems Program (BCS-0908549) funded the acquisition of the WorldView-2 satellite imagery. The authors wish to thank the Jack and Laura Dangermond Travel Scholarship's support of David Miller's travel to ICUC-10 / 14th Symposium on the Urban Environment.

References

Buyantuyev, A., Wu, J., 2009. Urbanization alters spatiotemporal patterns of ecosystem primary production: A case study of the Phoenix metropolitan region, USA. *J. Arid Environ*. 73, 512–520.

DeLucia, E.H., Drake, J.E., Thomas, R.B., Gonzalez-Meler, M., 2007. Forest carbon use efficiency: Is respiration a constant fraction of gross primary production? *Glob. Chang. Biol.* 13, 1157–1167.

Fissore, C., Baker, L.A., Hobbie, S.E., King, J.Y., McFadden, J.P., Nelson, K.C., Jakobsdottir, I., 2011. Carbon, nitrogen, and phosphorus fluxes in household ecosystems in the Minneapolis-Saint Paul, Minnesota urban region. *Ecol. Appl.* 21, 619–639.

Hilker, T., Coops, N.C., Wulder, M.A., Black, T.A., Guy, R.D., 2008. The use of remote sensing in light use efficiency based models of gross primary production: A review of current status and future requirements. *Sci. Total Environ.* 404, 411–423.

Hiller, R. V., McFadden, J.P., Kljun, N., 2011. Interpreting CO2 Fluxes Over a Suburban Lawn: The Influence of Traffic Emissions. *Boundary-Layer Meteorol.* 138, 215–230.

Imhoff, M.L., Bounoua, L., DeFries, R., Lawrence, W.T., Stutzer, D., Tucker, C.J., Ricketts, T., 2004. The consequences of urban land transformation on net primary productivity in the United States. *Remote Sens. Environ*. 89, 434–443.

Menzer, O., McFadden, J.P., 2017. Statistical partitioning of a three-year time series of direct urban net CO 2 flux measurements into biogenic and anthropogenic components. *Atmos. Environ.* 170, 319–333.

Milesi, C., Elvidge, C.D., Nemani, R.R., Running, S.W., 2003. Assessing the impact of urban land development on net primary productivity in the southeastern United States. *Remote Sens. Environ.* 86, 401–410.

Monteith, J.L., 1972. Solar radiation and productivity in tropical ecosystems. *J. Appl. Ecol.* 9, 747–766.

Nowak, D.J., Crane, D.E., Stevens, J.C., Hoehn, R.E., Walton, J.T., Bond, J., 2008. A Ground-Based Method of Assessing Urban Forest Structure and Ecosystem Services. *Arboric. Urban For.* 34, 347–358.

Nowak, D.J., Crane, D.E., Stevens, J.C., 2006. Air pollution removal by urban trees and shrubs in the United States. *Urban For. Urban Green*. 4, 115–123.

Oke, T.R., 1989. The micrometeorology of the urban forest. *Philos. Trans. R. Soc. B Biol. Sci.* 324, 335–349.

Peters, E.B., McFadden, J.P., 2012. Continuous measurements of net CO_2 exchange by vegetation and soils in a suburban landscape. *J. Geophys. Res. Biogeosciences* 117, G03005.

Peters, E.B., McFadden, J.P., 2010. Influence of seasonality and vegetation type on suburban microclimates. *Urban Ecosyst.* 13, 443–460.

Running, S.W., Zhao, M., 2015. User's Guide Daily GPP and Annual NPP (MOD17A2/A3) Products NASA Earth Observing System MODIS Land Algorithm Version 3.0 for Collection 6.

Sims, D.A., Luo, H.Y., Hastings, S., Oechel, W.C., Rahman, A.F., Gamon, J.A., 2006. Parallel adjustments in vegetation greenness and ecosystem CO2 exchange in response to drought in a Southern California chaparral ecosystem. *Remote Sens. Environ.* 103, 289–303.

Wu, J., Bauer, M.E., 2012. Estimating net primary production of turfgrass in an urban-suburban landscape with QuickBird imagery. *Remote Sens.* 4, 849–866.

Yuan, W., Liu, S., Zhou, G., Zhou, G., Tieszen, L.L., Baldocchi, D., Bernhofer, C., Gholz, H., Goldstein, A.H., Goulden, M.L., Hollinger, D.Y., Hu, Y., Law, B.E., Stoy, P.C., Vesala, T., Wofsy, S.C., 2007. Deriving a light use efficiency model from eddy covariance flux data for predicting daily gross primary production across biomes. *Agric. For. Meteorol.* 143, 189–207.

Zhao, T., Brown, D.G., Bergen, K.M., 2007. Increasing Gross Primary Production (GPP) in the Urbanizing Landscapes of Southeastern Michigan. *Photogramm. Eng. Remote Sens.* 73, 1159–1167.

Evaluation of uWRF Performance and Modeling Guidance Based on WUDAPT and NUDAPT UCP Datasets for Hong Kong

Introduction

The urban Weather Research and Forecasting Model (uWRF) (WRF BEP/BEM, Salamanca et al., 2010) has been widely used to study the urban boundary layer physics of several major cities. However, its performance in modeling Hong Kong and the Pearl River Delta (PRD) region has received less attention. One reason is the lack of a complete regional dataset of urban canopy parameters (UCPs), i.e. the National Urban Data and Access Portal Tool (NUDAPT) (Ching et al., 2009). The World Urban Database and Access Portal Tools (WUDAPT) (Ching et al., 2014) approach provides an alternative estimation of building morphology dimensions based on satellite-retrieved local climate zones (LCZs) (Stewart et al., 2012). Such an approach provides a simple open source means of generating the input data required for uWRF modeling. The implementation of WUDAPT in uWRF simulation involves uncertainties that arise from various sources, as compared with the NUDAPT approach in which more accurate building data are used.

These uncertainties include the following.

(1) The supervised classification of different LCZs in the WUDAPT approach by satellite images introduces uncertainty in identifying the correct LCZs.

(2) Given that the current WUDAPT approach based on LCZs requires selecting UCPs from a range of values associated with each LCZ, the choices may not accurately represent local conditions, thus introducing some degree of uncertainty into the modeling results.

(3) As the WUDAPT approach divides urban grids into classes (LCZs), compared with the continuous UCPs of the NUDAPT approach, this discretization introduces another source of uncertainty.

(4) The subsampling of WUDAPT and NUDAPT datasets into the uWRF's domain also generates uncertainty.

The quantification of these sources of uncertainty can improve the understanding of the efficacy of the WUDAPT model compared with the results from using NUDAPT-based UCP values. Some uncertainties could be reduced. Identifying the source of relatively large but reducible uncertainty could provide a framework and guidance for other regions, thus contributing to progress in the development of next-generation WUDAPT levels 1 and 2 datasets, which are more accurate than the current WUDAPT level 0.

In this study, different methods of WUDAPT level 0 preprocessing methods are carried out to isolate the source of uncertainties (1) to (4) above. The corresponding WRF result is compared with NUDAPT, which acts as the baseline "reference"; the extent of deviation of the WUDAPT cases vis à vis the NUDAPT case provides the means to quantify different sources of uncertainty.

After quantifying those different sources of uncertainty, we offer guidance for implementing WUDAPT in uWRF to possibly minimize uncertainty. Then we evaluate the improvement in the performance of uWRF with NUDAPT, along with the corresponding and suggested WUDAPT approach as input, for comparison with the traditional Noah bulk scheme and local and non-local planetary boundary layer (PBL) schemes, by considering surface observation station data.

Study area and experiment setup

Four typical calm wind days (December 18 to December 22, 2010) with a one-day spin-up (December 18) were chosen as the study period, when the urban effect was relatively dominant. In the simulations, a total of five domains with horizontal resolution of 27 km (domain 1), 9 km (domain 2), 3 km (domain 3), 1 km (domain 4), and 500 m (domain 5) were configured respectively. Domain 5, covering Hong Kong, was the area of interest in this study. To evaluate the performance of WUDAPT in uWRF applications compared with NUDAPT, and to quantify the different sources of uncertainty, we performed a set of experiments for domain 5. The setups of each experiment and their purposes are listed below. All of the cases share the same initial and boundary conditions and domain size, as inherited from domain 4. The only differences between them are the urban scheme, the PBL scheme, and the UCPs dataset used.

Case 1: NoahACM2.

In this case, for the PRD region the Noah bulk urban scheme was selected with the non-local ACM2 PBL scheme as recommended by Xie et al. (2012).

Purpose: To determine whether a more appropriate PBL scheme or an urban scheme is more important in simulation over an urban area.

Case 2: NoahBoulac.

In this case, the Noah bulk urban scheme was selected with a local Boulac PBL scheme that was a consistent PBL scheme for the WRF BEP/BEM model for a fairer comparison, because ACM2 is currently incapable of coupling with the BEP/BEM schemes in uWRF.

Purpose: As a control to demonstrate the improvement of the WRF BEP/BEM multi-layer urban scheme compared with the bulk scheme.

Case 3: BEPreal.

In this case, only the BEP was turned on with the Boulac PBL scheme with NUDAPT-type data in Hong Kong.

Purpose: To determine whether WRF BEP (without anthropogenic heating) performs better than the Noah bulk scheme. This case can also act as a reference to quantify the uncertainties from different WUDAPT Cases 5 to 10.

Case 4: BEPcat.

In this case, the continuous building morphology data (NUDAPT) were discretized into six categories based on the LCZs 1–6 criteria.

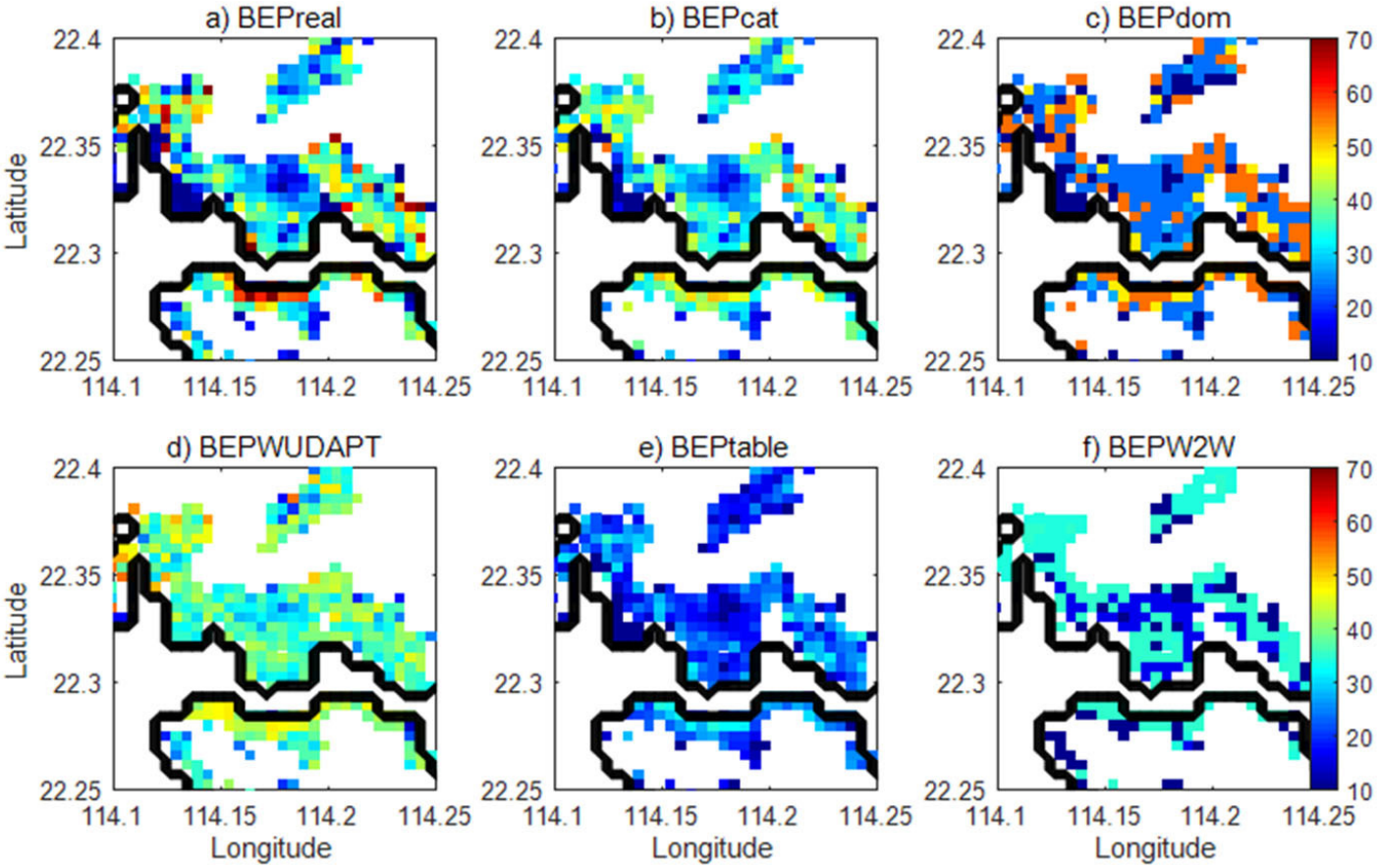

Figure 1. The zoomed-in spatial distribution of average building height [m] in Hong Kong for different cases. a) corresponds to case 3 and b) to f) correspond to cases 4-8.

Purpose: To quantify the uncertainty (by comparison with the reference case BEPreal) generated by discretizing continuous building morphology data. Given a distribution of real building morphology data (NUDAPT UCPs), how much uncertainty is generated by the simplification of these distributions by classifying them into LCZs?

Case 5: BEPdom

In this case, the data in BEPcat were subsampled on a dominant category basis rather than by subgrid averaging (Hammerberg et al., 2018, as indicated in Figure 5 and mentioned in section 3.3). Except for this case and Case 8, all of the other cases were performed based on a subgrid-averaging method.

Purpose: To quantify the uncertainty (by comparison with the reference case BEPreal) generated by the subsampling method (dominant vs. subgrid-averaging approach).

Case 6: BEPWUDAPT.

In this case, the WUDAPT dataset was fused with the NUDAPT categories in Case 4 (BEPcat) as the input data. The WUDAPT level 0 LCZs generated from the supervised classification method in Hong Kong was used with the UCP values (look-up table for Hong Kong) generated in Case 4 (BEPcat). In this way, the uncertainty was a sum of supervised classification method (machine-learning algorithm) and categorization (as in Case 5) because the look-up table values from Stewart and Oke (2012) were not used.

Purpose: To quantify the uncertainty (by comparison with the ground-truth) generated by the supervised classification method.

Case 7: BEPtable.

In this case, the UCPs in Case 4 (BEPcat) were replaced by look-up table values (Stewart & Oke, 2012). The uncertainty involved in this case was generated by the look-up table values, as the supervised classification (WUDAPT level 0 data) was not involved. The LCZs were derived from the actual building database in Case 3 (BEPreal).

Purpose: To quantify the uncertainty (by comparison with the ground-truth) generated by the lack of local information.

Case 8: BEPW2W.

In this case, the W2W protocol was used with WUDAPT level 0 LCZ data, and all of the uncertainties were involved.

Purpose: To examine the difference between the WRF output from the NUDAPT-type dataset and the WUDAPT dataset when all of the uncertainties are added up.

Case 9: BEPBEMreal.

In this case, both the BEP and BEM were turned on with the Boulac PBL scheme with NUDAPT-type data and the default setting for thermal properties in Hong Kong.

Purpose: To determine whether WRF BEPBEM (with default thermal settings) performs better than the WRF BEP alone.

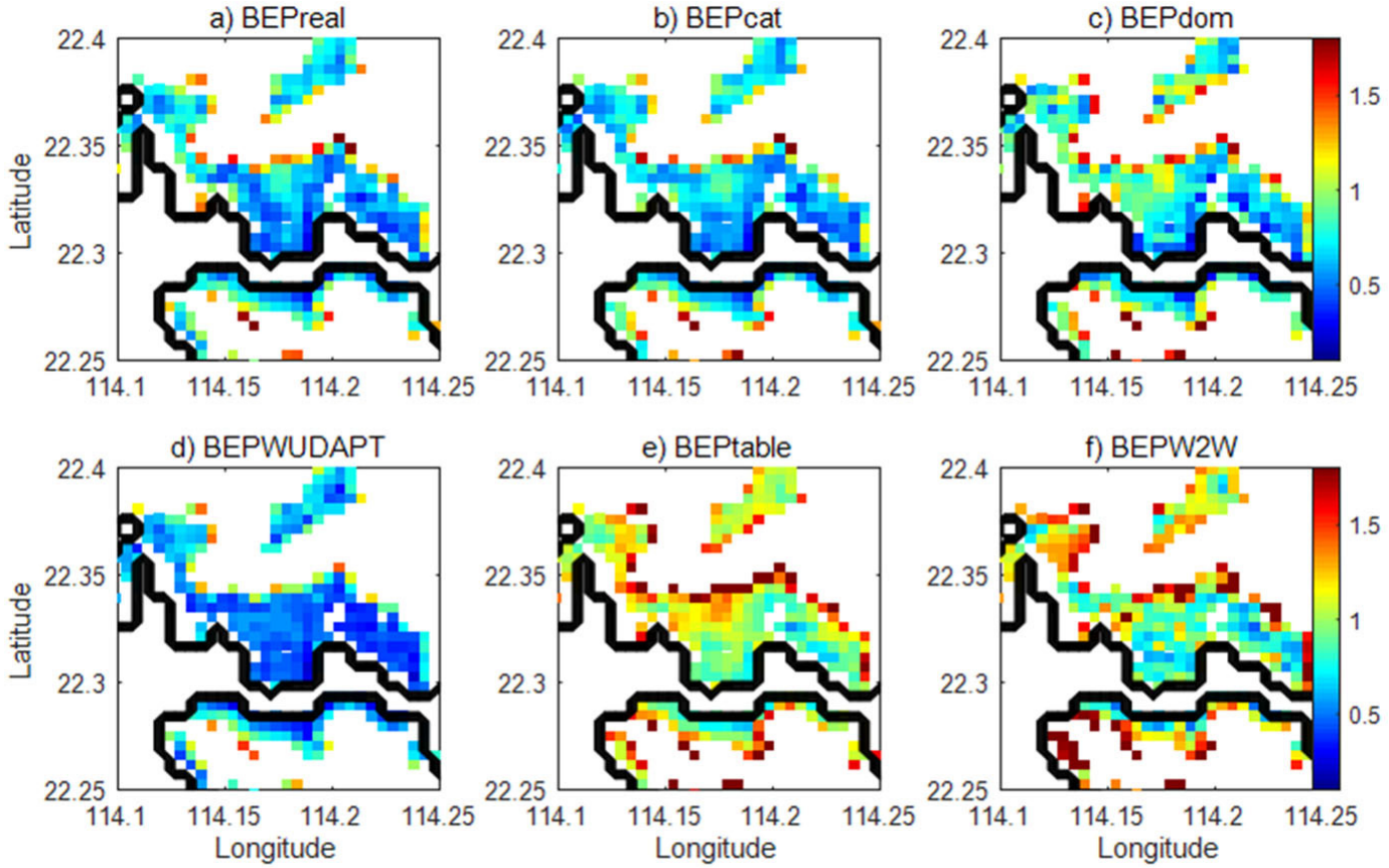

Figure 2. Corresponding averaged urban surface wind speed [m/s] of the NUDAPT case and different WUDAPT cases.

Simulation results

A. Comparison of the NUDAPT case and WUDAPT cases (Uncertainty from Different Cases).

Figure 1 and 2 show the zoomed-in (Kowloon Peninsula and Hong Kong Island) spatial distribution of input UCPs (average building height, A_h) and the corresponding output meteorological field (wind speed) for the NUDAPT case and the various WUDAPT cases. Spatially, the categorization (BEPcat) shows the closest A_h to the real case; the other cases all show greater differences. Furthermore, by using the dominant subsampling method (BEPdom) or the default W2W (Case 8, BEPW2W), the UCP input is more discrete because the dominant LCZs are considered for each modeling grid. In contrast, by using the look-up table by Brousse et al. (2016), the building height is severely underestimated because the buildings in European countries are generally shorter than those in Hong Kong. When the WUDAPT level 0 dataset is used along with the Hong Kong look-up table derived from BEPcat (BEPWUDAPT), the average building height is generally overestimated compared with the real case (mean deviation of 11m for the whole of Hong Kong), which suggests that the supervised classification algorithm tends to recognize more LCZ 1 and LCZ 4 (high-rise) categories in Hong Kong, as has been reported in other studies (Cai et al., 2016).

In Figure 2, as expected, it is visually evident that the deviation of BEPcat from BEPreal is smallest (0 m/s on average over the entire domain) regarding the magnitude and spatial pattern. This is the case because the only uncertainty involved, when compared with the real case, is the discretization of the UCPs from the NUDAPT type (continuous field) into the WUDAPT type (categories). This small difference can be related to Figures 1a and 1b in which the input UCPs for BEPcat is also very similar to the one in BEPreal (similar to other UCPs that are not shown here). The deviation of surface urban wind speed from the real case starts increasing when other sources of uncertainty become involved. The BEPdom case deviates on average 0.17 m/s from BEPreal over the whole urban area and can be up to 0.8 m/s or more in the zoomed-in region as shown in Figure 2. For example, in the highly dense Kowloon peninsula area, BEPreal estimated a surface wind speed of about 0.2 m/s, whereas BEPdom estimated around 1 m/s on average for the 3-day simulation period. This overestimation of surface wind speed suggests that the dominant LCZs approach generally leads to underestimates of the building height for the case of Hong Kong. This uncertainty arises from the considerable heterogeneity of the UCPs distribution in Hong Kong; subgrid tall building clusters can be ignored if the dominant type of buildings is relatively short. Subgrid averaging is preferable for minimizing this uncertainty because modelers can more or less control it via subsampling algorithms, compared with other sources of uncertainties.

Table 1: Averaged RMSE and BIAS for wind speed and temperature in different cases.

Cases		BEPreal	BEPBEMreal	BEPWUDAPT	NoahACM2	NoahBoulac
WIND [m/s]	RMSE	0.94	0.97	1.09	1.54	1.6
	BIAS	-0.44	-0.25	-0.61	0.74	0.57
TEMPERATURE [°C]	RMSE	1.36	1.43	1.41	1.5	1.52
	BIAS	-0.12	-0.03	0.03	-0.31	-0.41

For the BEPWUDAPT case, Figure 2d shows that spatially there is a general underestimation of urban surface wind speed because the supervised classification causes a misrecognition of LCZs (LCZ 1 and LCZ 4), which overestimate the building height and plan area ratio and thus increase urban drag. This suggests that an improvement of the WUDAPT level 0 data might be required for high-density urban areas such as Hong Kong, which deserves attention for level 1 and level 2 data with a better algorithm or the complement of different data sources (e.g., crowdsourcing, higher resolution satellite images). Furthermore, if the default look-up table is used (BEPtable in Figure 2e), the uncertainty is greatest among all the cases because local information (a localized look-up table) is lacking. Finally, for the default BEPW2W, spatially the uncertainty is similar to that in the BEPtable case and greater than in all of the other cases. A similar conclusion is drawn from the statistics for the whole of Hong Kong (domain 5), which are not shown here.

B. Improvement of WRF-BEP/BEM Compared with the Noah Bulk Scheme

Table 1 shows different averaged statistics of the models for a comparison of the observations in the BEP cases and The Noah bulk scheme cases. The following points can be made regarding improvements in surface wind speed simulation:

1. BEP's wind speed performs better than the Noah bulk scheme in terms of RMSE (from about 1.6 m/s for NoahBoulac to 0.94 m/s for BEPreal), regardless of whether WUDAPT or NUDAPT datasets are used, and it is similar to the BEP/BEM module (RMSE of 0.97 m/s). The magnitude of bias for BEPreal (-0.44 m/s) and BEPBEMreal (-0.25 m/s) is also smaller than that of NoahACM2 (0.74 m/s) and NoahBoulac (0.57 m/s). BEPWUDAPT has a magnitude of bias (-0.61 m/s) comparable with NoahBoulac because BEPWUDAPT overestimates the plan area ratio and building height of the urban area due to the uncertainty generated by the supervised classification of WUDAPT level 0 dataset (misrecognition of LCZs).

2. ACM2 performs better than the Boulac scheme in terms of RMSE, as demonstrated by Xie et al. (2012).

3. Over urban areas, the urban scheme overrides the impact of the PBL scheme because BEPreal, BEPBEMreal, and BEPWUDAPT perform better than ACM2-Noah in terms of RMSE.

4. BEM is not necessarily better than BEP alone, probably because of the lack of urban fraction data, thermal properties, and detailed anthropogenic heating data, all of which deserve further research on the WUDAPT level 1 and level 2 dataset that is currently under active development by the WUDAPT team.

With the non-local PBL scheme ACM2, the wind speed is higher in the daytime because of a better simulation of the non-local effect. The underestimation of wind speed for uWRF runs (WUDAPT/NUDAPT cases) in the daytime suggests a future need to couple the BEP/BEM urban scheme with a non-local scheme to better simulate the convective atmosphere.

Conclusions

This study evaluates the performance of the WRF BEP/BEM model in Hong Kong, which has unique hilly topographic conditions and landscape features with a highly inhomogeneous building morphology. The results show that combined with the multi-layer WRF BEP/BEM urban scheme (uWRF), the model gives a better simulation of wind speed and a slight improvement in the simulation of temperature over the urban area, in the context of urban sites. This indicates that the choice of a multi-layer urban scheme's benefit dominates the non-local PBL scheme's benefit in determining the quality of a surface simulation over an urban area, which is crucial for urban climate studies. Furthermore, different methods of implementing WUDAPT datasets in this study quantified the different sources of uncertainty. The ascending order for the uncertainty is as follows: 1) data discretization; 2) the dominant-type subsampling method, comparable with supervised classification in WUDAPT; and 3) the lack of local information (look-up tables). A compensation error may occur when all of the uncertainties accumulate in the W2W protocol, but the error in the region with maximum uncertainties is still the largest compared with other cases. However, WUDAPT is still a suitable alternative in regions where NUDAPT-type datasets are not available, provided that building morphology for different LCZs is estimated based on local expertise (assisted by the help of 3D maps) with a subgrid-averaging approach. BEM is not necessarily better than BEP alone, probably because of the lack of urban fraction data, thermal properties, and detailed anthropogenic data. This suggests the need of level 1 and level 2 WUDAPT datasets that give more detailed input for driving the BEP model.

Further work

Regarding directions for future study, the development of level 1 and level 2 WUDAPT datasets is crucial to further minimize sources of uncertainty. This may be accomplished by incorporating more and higher resolution satellite images in the supervision classification of LCZs or by improving the machine-learning algorithm, which is an ongoing effort for the WUDAPT team, as in the work of Xu et al. (2017). Besides building morphology data, more work is also needed to arrive at better estimations of buildings' thermal properties and the urban green fraction, based on building uses. Higher resolution satellite images may also provide more adequate information for repeating the current experiments of the BEM scheme. Coupling the uWRF schemes with a non-local PBL scheme is also expected to produce a better simulation in the context of convective conditions.

Acknowledgement

The study is supported by the RGC Grants 16300715 and 14611015 respectively. It is also partially supported by The Vice-Chancellor's Discretionary Fund of The Chinese University of Hong Kong. The authors would like to thank Miss Xinwei Li and Dr. Yong Xu for their help on training sample collection and the LCZ map development. We also appreciate the assistance of the Hong Kong Observatory (HKO), which provided the meteorological data.

References

Brousse, O., Martilli, A., Foley, M., Mills, G., & Bechtel, B. (2016). WUDAPT, an efficient land use producing data tool for mesoscale models? Integration of urban LCZ in WRF over Madrid. *Urban Climate*, 17, 116-134.

Cai, M., Ren, C., Xu, Y., Dai, W., & Wang, X. M. (2016). Local Climate Zone Study for Sustainable Megacities Development by Using Improved WUDAPT Methodology–A Case Study in Guangzhou. *Procedia Environmental Sciences*, 36, 82-89.

Ching, J., Brown, M., Burian, S., Chen, F., Cionco, R., Hanna, A., ... & Williams, D. (2009). National Urban Database and Access Portal Tool (NUDAPT): Facilitating a new generation of advanced urban meteorology and climate modeling with community-based urban database system. *Bulletin of the American Meteorological Society*.

Ching, J., See, L., Mills, G., Alexander, P., Bechtel, B., Feddema, J., Oleson, K. L., Stewart, I., Neophytou, M., Chen, F., Wang, X., & Hanna., A. (2014). WUDAPT: Facilitating advanced urban canopy modeling for weather, climate and air quality applications.

Hammerberg, K., Brousse, O., Martilli, A., & Mahdavi, A. (2018). Implications of employing detailed urban canopy parameters for mesoscale climate modelling: a comparison between WUDAPT and GIS databases over Vienna, Austria. *International Journal of Climatology*, 38, e1241-e1257.

Salamanca, F., Krpo, A., Martilli, A., & Clappier, A. (2010). A new building energy model coupled with an urban canopy parameterization for urban climate simulations—part I. formulation, verification, and sensitivity analysis of the model. *Theoretical and applied climatology*, 99(3-4), 331.

Stewart, I. D., & Oke, T. R. (2012). Local climate zones for urban temperature studies. *Bulletin of the American Meteorological Society*, 93(12), 1879-1900.

Xie, B., Fung, J. C., Chan, A., & Lau, A. (2012). Evaluation of nonlocal and local planetary boundary layer schemes in the WRF model. *Journal of Geophysical Research: Atmospheres*, 117(D12).







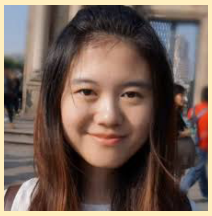


Michael Mau Fung Wong[1], Jimmy Chi Hung Fung[1,2], Jason Ching[3], Peter Pak Shing Yeung[1], Jason Wai Po Tse[4], Ran Wang[5], Meng Cai[5], Chao Ren[6,7]

[1] Division of Environmental and Sustainability, The Hong Kong University of Science and Technology, Hong Kong (michaelwong22mu@gmail.com); [2] Department of Mathematics (HKUST); [3] Institute for the Environment, University of North Carolina, Chapel Hill NC, USA; [4] Environmental Science Program (HKUST); [5] School of Architecture, The Chinese University of Hong Kong; [6] Hong Kong Faculty of Architecture, The University of Hong Kong; [7] Institute of Future Cities (CUHK)

Selection and application of appropriate thermal indices for urban studies

Introduction

Thermal bioclimate, or the general set of factors influencing human thermal stress, is concerned with contingency planning, protection of health, regional and urban planning, design of open spaces, various aspects of tourism and recreation areas, and research in climate change. It contributes to heat warnings and medical issues in weather forecasting. All these facets require a rational, thermo-physiologically consistent assessment of the human thermal environment. This is frequently accomplished by applying thermal indices. There is a long and extended discussion in human biometeorology about such thermal indices and which of them is the best and the most appropriate (Potchter et al., 2018; Staiger et al., 2019).

A methodical framework has been applied for the selection of thermal indices for applications in human biometeorological studies, especially in weather forecasting and, above all, urban issues such as the classification and quantification of open spaces or recreation areas. The method is explained in principle and is applied to the specific problem of an assessment of the human thermal environment. The results of this study especially contribute to the VDI guideline 3787/2 on "methods for the human biometeorological evaluation of climate for urban and regional planning" currently under revision (Staiger et al., 2019).

Appropriate thermal indices

There are more than 165 thermal indices and simulation devices that have been developed and applied during the last 100 years, designed to assess the thermal environment according to human thermal physiology and sensation (Staiger et al., 2019). From these, we selected the suitable indices for the thermophysiologically relevant quantification of the atmospheric environment. This provides the basis for the different human biometeorological applications for assessing the short-term impacts of weather and the long-term development of climate.

Recent studies also show the relevance of thermal indices and their justification to thermal perception. Only twelve out of 165 indices of human thermal perception are classified to be principally suitable for the human biometeorological evaluation of climate for urban and regional planning: this requires that the thermal indices provide an equivalent air temperature of an isothermal reference with minor wind velocity. Furthermore, thermal indices must be traceable to complete human energy budget models consisting of both a controlled passive system (heat transfer between body and environment) and a controlling active system, which provides a positive feedback on temperature deviations from neutral conditions of the body core and skin as is the case in nature. Seven out of the twelve indices are fully suitable, out of which three overlap with the others. Accordingly, the following four indices were selected as appropriate: Universal Thermal Climate Index (UTCI), Perceived Temperature (PT), Physiologically Equivalent Temperature (PET), and rational Standard Effective Temperature (SET*), and an option for a fifth index is also given (mPET).

1. UTCI, the Universal Thermal Climate Index: UTCI refers to an isothermal environment, with calm air (v ~0.3 m/s at 1.1 m above ground) and RH = 50% at Ta = 29°C (or at higher air temperature with a fixed water vapor pressure of 20 hPa, which is equivalent to 50% at 29°C). The reference subject's net metabolic heat production, M-W, is assumed to be 135 W/m^2. The basic thermoregulatory model is the "UTCI-Fiala multi-node model (187 nodes) of human heat transfer and temperature regulation". It is combined with a clothing ensemble as worn by a general population with a realistic insulation distributed over the different body segments. The clothing insulation is behaviorally adapted dependent on Ta; the heat and humidity resistance of clothing is a function of v and the reference subject's movement (4 km/h), i.e. the overall insulation usually differs between the reference environment defined for calm air and the actual environment. The operational UTCI procedure is a laborious parameterization of the basic models, combining the precision of complex multi-node models with low computational costs.

2. PT, the Perceived Temperature: PT refers to an isothermal environment where v is reduced to a slight draught enabling forced convection and RH = 50%. The reference subject's M-W (metabolism-activity) is assumed to be 135 W/m^2, and in terms of thermophysiology, PT is constituted by PMV (Predicted Mean Vote) and PMV*, which it converts to an equivalent temperature. Fanger's PMV is applied as restricted to the comfort zone, and enables behavioral adaptation. This behavioral adaptation is realized by varying the intrinsic clothing insulation between a winter value (Icl = 1.75 clo), and a summer value (Icl = 0.5 clo) for the clothing ensemble, and requiring that PMV equals zero. Here, the insulation is identical in both the actual and reference environment. Outside the comfort zone, PMV* is calculated as anchored on the two boundary values for the variable insulation zone, which results in two parameterizations of the ASHRAE two-node model so as to obtain realistic values of skin temperature, Tsk, core temperature, Tcr, and skin wettedness w, to be used for PT. The computational costs for PT are low due to the parameterizations as well as Fanger's relatively simple comfort equation for steady state (Fanger, 1972).

3. PET, the Physiologically Equivalent Temperature: PET is equal to Ta in an environment that is assumed as a typical isothermal indoor setting, with v= 0.1 m/s at 1.1 m above ground and a water vapor pressure of 12 hPa (50% RH at 20°C). The reference subject is assumed to perform light

activity (80 W work metabolism, corresponding to M-W of 83.7 W/m^2) and wear a clothing ensemble with Icl = 0.9 clo. In terms of thermophysiology, PET is based on the Munich Energy-balance Model for Individuals, MEMI. MEMI is a two-node model and differs largely "from the Gagge two-node model (Gagge et al., 1986) by calculating the physiological sweat rate as a function of Tsk and of Tcr and by the separate calculation of heat flows from parts of the body surface that are covered or uncovered by clothing". MEMI offers an analytical solution of the human energy balance for steady state and avoids temporal integration compared to transient models. Because of the dependence on Tsk and on Tcr, there are quadratic equations, among others, to be solved by iteration and where the sign in the solution is selected using bins of Tsk and Tcr with boundaries that are obviously set statistically. MEMI is applied unmodified in determining the thermophysiological state in the actual environment. Following this, PET as Ta of the reference environment is calculated by applying, unchanged, all heat exchanges of the actual environment, which are associated with the thermoregulatory control mechanisms of the actual environment, namely Tsk, w, the clothing surface temperature and the latent heat flow from evaporation of sweat. Then, Ta is iterated up to a balanced energy budget by adopting the meteorological settings of the reference environment. Hence, in a first approximation, PET is constructed in a way comparable to a standard operative temperature, and thus differs from the other two-node indices whose structure is comparable to a standard humid operational temperature.

4. SET*, the rational Standard Effective Temperature: SET* is originally defined for typical indoor environments and as Ta of an isothermal environment at still air and RH = 50%. In this environment, the reference subject, in steady state and wearing clothing with a standardized Icl for the activity concerned, has the same heat stress (Tsk) and thermoregulatory strain (w) as in the actual environment. A sedentary subject with M-W of 73 W/m^2, resulting in an intrinsic Icl of 0.6 clo, is assumed. In terms of thermophysiology, SET* is based on the ASHRAE two-node model, which provides this index (as well as the rational Effective Temperature ET*) as standard output after a temporal integration of 120 one-minute steps.

5. A modified PET, mPET, has become available that retains the definition of the PET reference environment and the fundamental parts of the underlying thermophysiology, but improves both passive and active thermoregulation significantly (Chen and Matzarakis, 2018). This is achieved by applying an enhanced body model, by introducing conductive heat transfer inside the body and improving the heat transfer inside the body using Pennes' bio-heat equation (Pennes, 1948), and, above all, by accounting for up to three layers in the clothing model able to vary in heat and water vapor transfer coefficients and also for vapor condensation in the layers able to alter both the dry and the wet energy flux profiles. If this is done, clothing insulation adapts behaviorally to the actual Ta and is then applied identically to both environments, actual and reference. Because the model is semi-unsteady and can embrace up to 25 nodes, it requires up to 1200 time steps to produce the body temperature profiles and stable energy fluxes in order to finally solve the human heat balance equation for steady state and to calculate mPET. This increases the computational costs compared to the simpler PET two-node version. mPET fulfills all the requirements to be the fifth index, but more applications and validations are required.

This section summarizes the recently published paper: Staiger, H., Laschewski, G., Matzarakis, A., 2019. Selection of Appropriate Thermal Indices for Applications in Human Biometeorological Studies. *Atmosphere* 10(18) 1-15.

Calculation possibilities for thermal indices

RayMan and SkyHelios Model

The RayMan model (www.urbanclimate.net/rayman) was developed to calculate short wave and long wave radiation fluxes affecting the human body. The model considers complex building structures and is suitable for the analysis of the effect of various planning scenarios in different micro to regional scales. The model calculates the mean radiant temperature (Tmrt), which is required for the human energy balance model and, thus, for the assessment of human thermal bioclimate. The thermal indices Predicted Mean Vote, Standard Effective Temperature, Physiologically Equivalent Temperature, modified Physiologically Equivalent Temperature, Universal Thermal Climate Index and Perceived Temperature can be calculated (Matzarakis et al., 2007, 2010).

In addition, information about urban structures (buildings, deciduous and coniferous trees) can be generated or imported. Based on the input possibilities, sunshine duration with or without SVF, estimation of the daily mean, max or sum of global radiation or shadows for existing or future complex environments can be calculated. For the estimation of thermal indices, meteorological data can be entered through manual input or by loading data files. The output is provided as graphs and text files. RayMan offers the opportunity of importing long-term data sets of meteorological parameters allowing statistical assessments (Matzarakis et al., 2010).

For analysing the spatial dimension of micro climate the SkyHelios model (Fig. 1) has been developed (Matzarakis and Matuschek, 2011). The SkyHelios model (www.urban-climate.net/skyhelios) makes use of the graphics engine MOGRE to estimate climatological and human-biometeorological parameters. In detail, the spatial input is converted into a graphics scene with surface texture colors according to the surface material properties (shortwave albedo and longwave emission coefficient). Another color band is utilized to determine to what extent a surface is exposed to direct solar irradiation. This is not only used for display, but allows for the rendering of fisheye images containing the necessary input to estimate spatially resolved short- and longwave radiation fluxes, that are finally summarized in

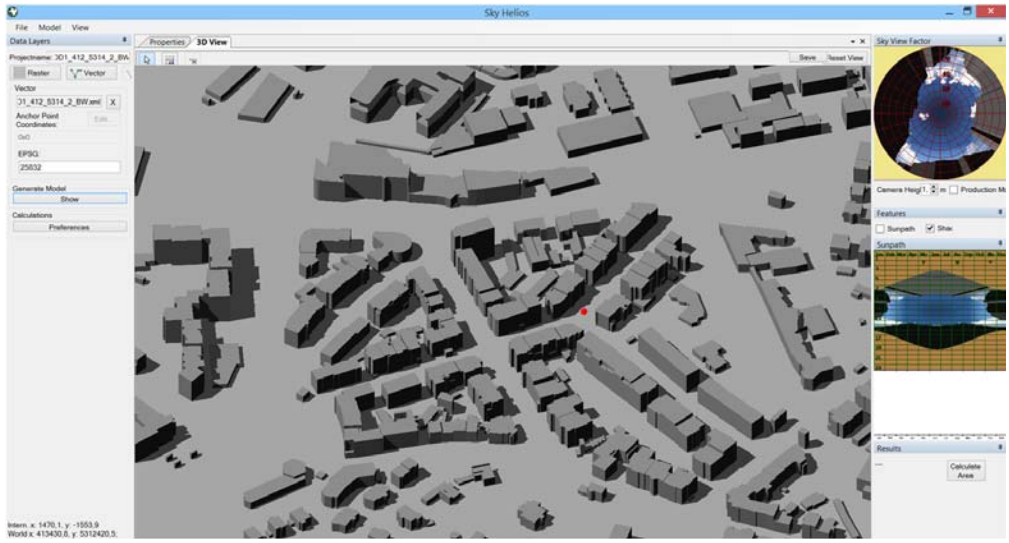

Figure 1. Shading at 14:34 LST calculated for an excerpt of the City of Freiburg, represented by a CityGML building geometry model using the SkyHelios model in display mode.

terms of the mean radiant temperature (Tmrt). SkyHelios can therefore be applied for modeling climate conditions or climate relevant parameters on the micro-scale with respect to complex morphologies.

Another important input parameter is wind speed (v). As well as Tmrt, v is hard to measure within urban areas. Therefore, a three dimensional diagnostic wind model was integrated into SkyHelios that allows for the determination of spatially resolved wind speed and direction. Using all this information together, SkyHelios is capable of estimating the thermal indices PET, PT and UTCI spatially resolved in high resolution (Matzarakis and Fröhlich, 2018, Fröhlich et al., 2018).

Conclusion

Four approaches UTCI, PT, PET and SET* and an option for a fifth one (mPET) are suitable for the aim of the thermophysiologically consistent assessment of the human thermal environment. The selected four indices will be included in the revised VDI guideline 3787/2. This will enable the user to select the suitable index for his specific purpose and to support his conclusions by comparison with the results of one of the other indices.

References

Chen, Y.-C., Matzarakis, A., 2018. Modified physiologically equivalent temperature – basics and applications for western European climate. *Theoretical and Applied Climatology*, 132: 1275-1289.

Chen, Y.-C., Fröhlich, D., Matzarakis, A., Lin, T-.P., 2017. Urban Roughness Estimation Based on Digital Building Models for Urban Wind and Thermal Condition Estimation—Application of the SkyHelios Model. *Atmosphere*, 8, 247.

Fanger, P.O., 1972. Thermal Comfort. Analysis and Applications in Environmental Engineering. McGraw-Hill Company, pp. 244.

Fröhlich, D., Matzarakis, A., 2018. Spatial Estimation of Thermal Indices in Urban Areas—Basics of the SkyHelios Model. *Atmosphere*, 9: 209, 1-14.

Fröhlich, D., Gangwisch, M., Matzarakis, A., 2019. Effect of radiation and wind on thermal comfort in urban environments - Application of the RayMan and SkyHelios model. *Urban Climate*, 27: 1-7.

Gagge, A.P., Fobelets, A.P., Berglund, P.E., 1986. A Standard Predictive Index of Human Response to the Thermal Environment. *ASHRAE Trans*., 92: 709–731.

Matzarakis, A., Rutz, F., Mayer, H., 2007. Modelling Radiation fluxes in simple and complex environments – Application of the RayMan model. *Intl. J. Biometeorol.*, 51: 323-334.

Matzarakis, A., Rutz, F., Mayer, H., 2010. Modelling Radiation fluxes in simple and complex environments – Basics of the RayMan model. *Intl. J. Biometeorol.*, 54: 131-139.

Matzarakis, A., Matuschek, O., 2011. Sky View Factor as a parameter in applied climatology – Rapid estimation by the SkyHelios Model. *Meteorologische Zeitschrift*, 20: 39-45.

Pennes, H.H., 1948: Analysis of tissue and arterial blood temperatures in the resting human forearm. *J. Appl. Physiol*., 85: 35–41.

Potchter, O., Cohen, P., Lin, T,.P., Matzarakis, A., 2018. Outdoor human thermal perception in various climates: A comprehensive review of approaches, methods and quantification. *Science of the Total Environment*, 631-632: 390-406.

Staiger, H., Laschewski, G., Matzarakis, A., 2019. Selection of Appropriate Thermal Indices for Applications in Human Biometeorological Studies. *Atmosphere*, 10: 18; 1-15.

Andreas Matzarakis

andreas.matzarakis@dwd.de

Research Centre
Human Biometeorology
German Meteorological Service
Freiburg, Germany

A Tribute to Professor Arieh Bitan (1935-2019)

Prof. Arieh Bitan was born in 1935 in Berlin and immigrated to Israel with his parents and two sisters in 1938. In 1957 he enrolled at the Hebrew University in Jerusalem, in the Department of Geography and the Department of Meteorology and Climatology. In 1960 he received his bachelor's degree *cum laude* and continued as a master's degree student in the Department of Geography, graduating with honors in 1963. As a doctoral student in that department he served as a teaching assistant and counselor, earning his doctorate in 1969. After advanced studies at the German Meteorology Service in urban climatology and topoclimatology, he became a lecturer in the Department of Geography of the Hebrew University.

In 1977 Prof. Bitan joined the Department of Geography and the Human Environment at Tel Aviv University, and established the Unit for Urban and Applied Climatology and Environmental Aspects.

Prof. Bitan studied at many foreign research institutes, among them Karlsruhe and Essen Universities, the Free University of Berlin, University of Arizona, University of New Mexico and San Jose State University in California. He has been an invited speaker to innumerable universities, research institutes and international conferences.

Prof. Bitan was one of the leading urban climatology researchers worldwide and among the founders of the International Association for Urban Climate (IAUC). He was a member of the Board from its inception in 2002 until 2006. From 1982-1995 he served as Head of the Expert Committee for Urban Climatology and Building Climatology of the International Federation for Housing and Planning (IFHP). In the years 1991-1995 he was a member of the steering committee of the Tropical Urban Climate Experiment (TRUCE) of the World Meteorological Organization (WMO) – and in the years 1991-1993 he was Vice Chairman of the International program Committee of the Technical Conference on Tropical Urban Climatology in Dhaka, Bangladesh, organized in 1993 by WMO, IFHP, CIB, and IGU. In 2005 he was invited to join the international research group of the World Health Organization (WHO) for improving public health responses to extreme weather (EuroHEAT).

In 1980 and 1983 he initiated two international conferences in Israel on urban climatology and climatic related planning, and chaired their organizing committees. These conferences were the foundation for establishing a regularly scheduled triennial congress on these topics, held in different venues around the world – today known as the International Conference on Urban Climate, organized under the auspices of the IAUC. Prof. Bitan has been a member of the organization or of the Scientific Committees for all the conferences that have been held since then. In addition, Prof. Bitan initiated and organized two international summer schools in 1992 and 1993 in the Department of Geography and the Human Environment of Tel Aviv University on the subject of urban and climatic related planning and building.

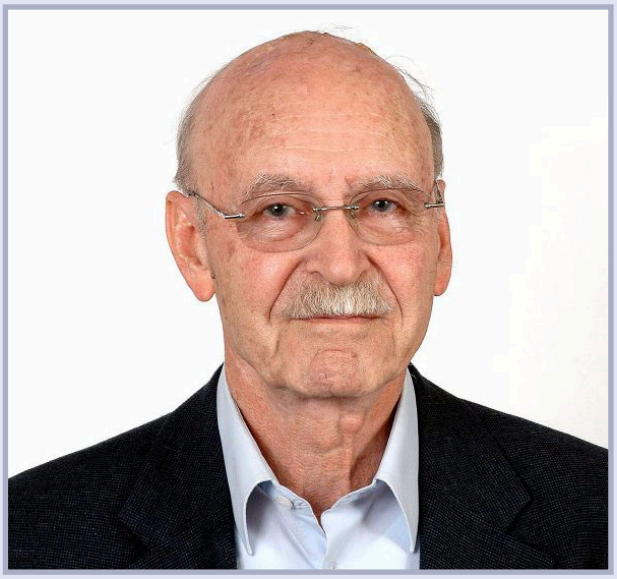

Prof. Bitan was among the leading climate researchers in Israel, and was the first to conduct regional topo-climatic studies in several of its regions – as well as to investigate the climatic conditions of the interior lakes of Israel (Dead Sea and Lake Kinneret-Sea of Galilee). The resulting data provided a strong basis and an important source of information when he served as the consultant for establishing the location and climatically-responsive building strategies of new cities and rural settlements in Israel. Among the first researchers in the field, Prof. Bitan was a leader in the study of urban climatology and climate-related urban planning in Israel – from the city level to that of the single house. He was the climatology advisor for the Ministry of Housing and Construction and the Ministry of National Infrastructures, as well as for the Israel Defense Forces Construction Center and many other planning and building bodies.

Prof. Bitan published dozens of articles in top-ranking international journals, and more than 90 research and consultation reports. In the years 1981, 1984, 1988 and 1991 he edited a series of four books on urban climatology and climatically related planning published by Elsevier Publishing, and was supervisor to about 30 master and doctoral students.

Prof. Bitan was twice the Head of the Department of Geography and the Human Environment at Tel Aviv University, in the years 1982-1987 and 1995-1998.

He received the IAUC's Luke Howard Award in 2006.

He will be sadly missed.

— *Hadas Saaroni, Tel Aviv University*

Urban Areas and Global Change sessions at the American Geophysical Union Fall Meeting in Washington, D.C., USA

By Joe McFadden (mcfadden@ucsb.edu)
University of California, Santa Barbara, USA

The 2018 American Geophysical Union (AGU) annual Fall Meeting, held in Washington, D.C., USA from December 10–14, was the largest ever with more than 28,500 attendees representing 101 different countries. According to the AGU, there were a total of 25,000 oral and poster presentations organized in some 1,900 scientific sessions. Among them was a series of sessions on Urban Areas and Global Change, convened by Prof. **Galina Churkina** (Yale University), Prof. **Joe McFadden** (University of California, Santa Barbara), Prof. **Lei Zhao** (University of Illinois, Urbana-Champaign), and **David Miller** and **Erin Wetherley** (University of California, Santa Barbara).

The Urban Areas and Global Change sessions invited submissions of new results based on observational, modeling, or data-driven studies of biogeochemical, biophysical, or ecological interactions of human-land-atmosphere systems in urban areas; and of socio-institutional and technological components affecting the spatial and temporal patterns of carbon emissions. The oral session, convened Wednesday afternoon in the middle of the conference week, was kicked off by **Burak Guneralp** (Texas A&M University) with his talk on *"A Synthesis on Four Decades of Global Urban Expansion: 1970-2010."* An invited talk was presented by **Eleanor Stokes** (NASA Goddard Space Flight Center) on *"Characterizing multiple dimensions of urban change"* using remotely-sensed nighttime lights data from the Visible Infrared Imaging Radiometer Suite (VIIRS) to understand urban land use and energy use, and to track infrastructure growth, alongside population and built environment transitions in Indian and American cities.

Urban vegetation, its stress conditions in cities, and its effects on outdoor thermal comfort, microclimate, and water fluxes were presented in talks by **Fang Fang** (West Virginia University), **Winston Chow** (National University of Singapore), and **Naika Meili** (Singapore-ETH Centre). Another group of talks focused on atmospheric processes across a range of scales, including building configuration and air pollutant exposure by **Liye Zhu** (Sun Yat-Sen University), and non-linear impacts of urban heat on atmospheric circulation by **Elie Bou-Zeid** (Princeton University).

On the morning following the oral session, there was a well-attended poster session in the cavernous hall of the Walter E. Washington Convention Center. Several posters examined vegetation effects in cities, including topics such as examining whether waste CO_2 from inside buildings could be used to enhance rooftop garden productivity (**Sarabeth Buckley**, Boston University), and whether shade trees in some cities and landscape positions could become a net source of CO_2 to the atmosphere (**Tedward Erker**, University of Wisconsin). Another group of posters used remote sensing to examine population, land use, and land cover, including urbanization dynamics (**Michelle Stuhlmacher**, Arizona State University). Several posters focused on urban energy budgets and the urban heat island effect over a global range of cities including New York City, Reno, Kansas City, several California cities, and the Eastern region of the USA; the Aburrá Valley, Colombia; and tropical cities in India.

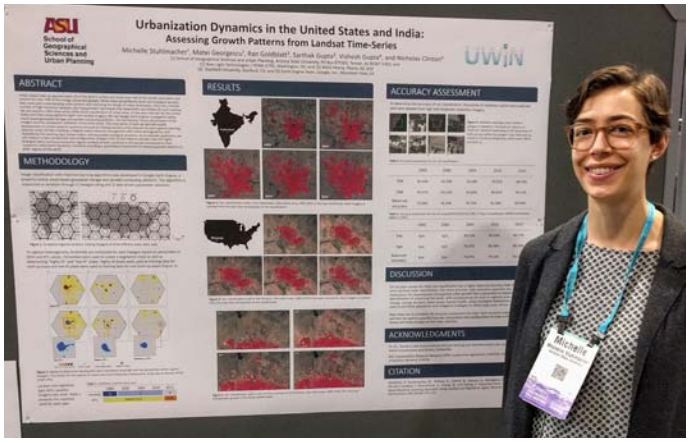

Michelle Stuhlmacher (Arizona State University) presented a poster of work using Google Earth Engine, nighttime light satellite data, and Landsat imagery to classify built-up areas in the United States and India.

Eleanor Stokes (NASA Goddard Space Flight Center) gave the invited presentation in the oral session on "Characterizing multiple dimensions of urban change".

The Urban Areas and Global Change sessions at the 2018 AGU Fall Meeting followed a multi-year series of similarly organized sessions over the past several years. The organizers indicated that they wish to continue this series at the 2019 AGU Fall Meeting, which will return to San Francisco at the newly renovated Moscone Center on December 9-13, 2019. They welcome the continued strong participation of the international urban climate community at the 2019 meeting.

First Global Forum on Heat and Health held in Hong Kong, China on December 17-20, 2018

By Lucas Scherdel[1], Joy Shumake-Guillemot[1], Hunter Jones[2], Juli Trtanj[2], and Chao Ren[3]

[1]World Health Organization/World Meteorological Organization, Climate and Health Office, Geneva, Switzerland (jshumake-guillemot@wmo.int)

[2]National Oceanic and Atmospheric Administration, Climate Program Office, Washington, D.C., USA

[3]The University of Hong Kong, Faculty of Architecture, Hong Kong, China

Panel discussion on engagement and communications.

Following consultations held in Chicago, USA (2015) and Colombo, Sri Lanka (2016), the **First Global Forum on Heat and Health** brought together more than 120 interdisciplinary experts and practitioners from 33 countries to strengthen cooperation in interdisciplinary science and practice to build the capacity of governments, organizations, and professionals to protect populations from the avoidable health risks of extreme and ambient heat.

The international forum also formally launched the **Global Heat Health Information Network** (http://www.ghhin.org/), an independent, voluntary, and member-driven forum of scientists, professionals, and policymakers focused on enhancing and multiplying the global and local learning regarding resilience building for heat health.

Worldwide experts agree that extreme hot weather is having devastating consequences for human health in all inhabited world regions. For many places, heat waves kill more people than any other weather-related disaster. Researchers in Hong Kong told the First Global Forum on Heat and Health that, in highly urbanized and densely populated parts of the Asian city, every 1°C increase in maximum daytime temperature above 28.2°C results in a 1.8% increase in mortality. Experts note that the world could reach a level of more than 80–90% urbanization by the last quarter of the century, placing extremely large populations at risk.


Participants in the Global Forum on Heat and Health.

Attendees participated in a simulated emergency exercise of a high impact heatwave event with many casualties where participants learned the effectiveness of timely, clear, and concise communication with the public, media, governments, and stakeholders to prevent and reduce health impacts. The forum launched a global network which will seek to build diverse partnerships, improve available evidence and actionable information for planning and preparedness, enhance global heat wave prediction capabilities, and promote life-saving heat-resilient interventions such as community outreach and early warning systems.

The diverse network of professionals from many fields—including medical doctors, meteorologists, architects, and urban designers—committed to work together to improve risk monitoring capabilities, including meteorological information and warnings, and health surveillance. Experts will share its recommendations with its partner organizations, including the World Meteorological Organization and World Health Organization, recognizing their importance in providing guidance for addressing these risks.

"The year 2018 was the fourth warmest year on record, one of 20 warmest years that have occurred in the past 22 years. Many parts of the world experienced exceptional heat, prolonged heatwaves, and associated wildfires," said Elena Manaenkova, WMO Deputy Secretary-General. "Hot extremes will increase in the future and so the risk to human health. Heat warnings and related weather and climate services are critical to mitigate this risk. Therefore, WHO and WMO are taking urgent action and bringing health experts and meteorologists together to enhance heat-health services to the public."

The Global Heat Health Information Network recommended that a Second Global Forum be held no later than 2020.

Recent Urban Climate Publications

Abatan A, Osayomi T, Akande SO, Abiodun BJ, Gutowski-Jr WJ (2018) Trends in mean and extreme temperatures over Ibadan, Southwest Nigeria. *Theoretical and Applied Climatology* 131(3-4) 1261–1272.

Ajaaj AA, Mishra AK, Khan AA (2018) Urban and peri-urban precipitation and air temperature trends in mega cities of the world using multiple trend analysis methods. *Theoretical and Applied Climatology* 132(1-2) 403–418.

Albano R, Sole A, Adamowski J, Perrone A, Inam A (2018) Using FloodRisk GIS freeware for uncertainty analysis of direct economic flood damages in Italy. *International Journal of Applied Earth Observation and Geoinformation* 73 220-229.

Ali-Toudert F, Böttcher S (2018) Urban microclimate prediction prior to dynamic building energy modelling using the TEB model as embedded component in TRNSYS. *Theoretical and Applied Climatology* 134(3-4) 1413–1428.

Angeles ME, González JE, Ramírez N (2018) Impacts of climate change on building energy demands in the intra-Americas region. *Theoretical and Applied Climatology* 133(1-2) 59–72.

Baraldi R, Neri L, Costa F, Facini O, Rapparini F, Carriero G (2019) Ecophysiological and micromorphological characterization of green roof vegetation for urban mitigation. *Urban Forestry & Urban Greening* 37 24-32.

Barnes ML, Welty C, Miller AJ (2018) Impacts of Development Pattern on Urban Groundwater Flow Regime. *Water Resources Research* 54 5198-5212.

Bartesaghi-Koc C, Osmond P, Peters A (2019) Mapping and classifying green infrastructure typologies for climate-related studies based on remote sensing data. *Urban Forestry & Urban Greening* 37 154-167.

Bauer TJ (2019) The Effect of the Urban Parametrization on Simulated Contaminant Atmospheric Transport and Dispersion. *Boundary-Layer Meteorology* 170 95–125.

Bechtel B, Alexander PJ, Beck C, Bцhner J, Brousse O, Ching J, Demuzere M, Fonte C, G6l T, Hidalgo J, others (2019) Generating WUDAPT Level 0 data–Current status of production and evaluation. *Urban Climate* 27 24–45.

Bisht DS, Chatterjee C, Raghuwanshi NS, Sridhar V (2018) An analysis of precipitation climatology over Indian urban agglomeration. *Theoretical and Applied Climatology* 133(1-2) 421–436.

Blackman K, Perret L, Savory E (2018) Effects of the Upstream-Flow Regime and Canyon Aspect Ratio on Nonlinear Interactions Between a Street-Canyon Flow and the Overlying Boundary Layer. *Boundary-Layer Meteorology* 169 537–558.

Brasseur GPZ, Xie Y, Petersen AK, Bouarar I, Flemming J,

In this edition is a list of publications that have generally come out between **December 2018 and February 2019**. If you believe your articles are missing, please send your references to the email address below with a header "IAUC publications" and the following format: Author, Title, Journal, Year, Volume, Issue, Pages, Dates, Keywords, URL, and Abstract. Important: do so **in a .bib format.**

Dr. Ashley Broadbent (School of Geographical Sciences & Urban Planning, ASU, US), who contributed to this community for more than 2 years, decided to resign from the Bibliography Committee. On behalf of the community I would like to thank him for his continuous support to this community.

Note that we are nevertheless always looking for (young) researchers to join and contribute to the Committee. If you are interested to join or would like to receive more information, please let me know via the email address below.

Regards,

Matthias Demuzere

Chair IAUC Bibliography Committee

Ruhr University Bochum (Germany)

Matthias.demuzere@rub.de

The Bibliography Committee

Lilly Rose Amirtham

Anurag Bagade

Pravin Bhiwapurkar

Peter Crank

Rohinton Emmanuel

Kathrin Feige

Lech Gawuc

Rafiq Hamdi

Julia Hidalgo

Martina Petralli

Iara Santos

Abel Tablada

Hendrik Wouters

Qunshan Zhao

Gauss M, Jiang F, Kouznetsov R, Kranenburg R, Mijling B, Peuch V-H, Pommier M, Segers A, Sofiev M, Timmermans R, van der Ronald A, Walters S, Xu J, Zhou G (2019) Ensemble forecasts of air quality in eastern China - Part 1: Model description and implementation of the Marco-Polo-Panda prediction system, version 1. *Geoscientific Model Development* 12 33-67.

Broadbent AM, Coutts AM, Nice KA, Demuzere M, Krayenhoff ES, Tapper NJ, Wouters H (2019) The Air-temperature Response to Green/blue-infrastructure Evaluation Tool (TARGET v1. 0): an efficient and user-friendly model of city cooling. *Geoscientific Model Development* 12 785–803.

Broadbent AM, Coutts AW, Tapper NJ, Demuzere M, Beringer J (2018) The microscale cooling effects of water sensitive urban design and irrigation in a suburban environment. *Theoretical and Applied Climatology* 134(1-2) 1–23.

Brousse O, Georganos S, Demuzere M, Vanhuysse S, Wouters H, Wolff E, Linard C, Nicole P-M, Dujardin S (2019) Using Local Climate Zones in Sub-Saharan Africa to tackle urban health issues. *Urban Climate* 27 227–242.

Buccolieri R, Santiago J-L, Rivas E, Sáanchez B (2019) Reprint of: Review on urban tree modelling in CFD simulations: Aerodynamic, deposition and thermal effects. *Urban Forestry & Urban Greening* 37 56-64.

Burgos AG, Hamlington BD, Thompson PR, Ray RD (2018) Future Nuisance Flooding in Norfolk, VA, From Astronomical Tides and Annual to Decadal Internal Climate Variability. *Geophysical Research Letters* 45 12432–12439.

Byun K, Chiu C-M, Hamlet AF (2019) Effects of 21st century climate change on seasonal flow regimes and hydrologic extremes over the Midwest and Great Lakes region of the US. *Science of The Total Environment* 650 1261-1277.

Cai B, Lu J, Wang J, Dong H, Liu X, Chen Y, Chen Z, Cong J, Cui Z, Dai C, Fang K, Feng T, Guo J, Li F, Meng F, Tang W, Wang G, Xie Y, Zhang J (2019) A benchmark city-level carbon dioxide emission inventory for China in 2005. *Applied Energy* 233 659-673.

Chakraborty T, Lee X (2019) A simplified urban-extent algorithm to characterize surface urban heat islands on a global scale and examine vegetation control on their spatiotemporal variability. *International Journal of Applied Earth Observation and Geoinformation* 74 269-280.

Chen P-C, Alvarado V, Hsu S-C (2018) Water energy nexus in city and hinterlands: Multi-regional physical input-output analysis for Hong Kong and South China. *Applied Energy* 225 986-997.

Chen S, Xu B, Chen B (2018) Unfolding the interplay between carbon flows and socioeconomic development in a city: What can network analysis offer? *Applied Energy* 211 403-412.

Chen Y, Hong T, Luo X, Hooper B (2019) Development of city buildings dataset for urban building energy modeling. *Energy and Buildings* 183 252 - 265.

Chen YC, Matzarakis A (2018) Modified physiologically equivalent temperature—basics and applications for western European climate. *Theoretical and Applied Climatology* 132(3-4) 1275–1289.

Cheng J, Qi DH, Katal A, Wang LZ, Stathopoulos T (2018) Evaluating wind-driven natural ventilation potential for early building design. *Journal of Wind Engineering and Industrial Aerodynamics* 182 160–169.

Chi X, Li R, Cubasch U, Cao W (2018) The thermal comfort and its changes in the 31 provincial capital cities of mainland China in the past 30 years. *Theoretical and Applied Climatology* 132(1-2) 599–619.

Chini CM, Stillwell AS (2018) The State of US Urban Water: Data and the Energy-Water Nexus. *Water Resources Research* 54 1796-1811.

Claude S, Ginestet S, Bonhomme M, Escadeillas G, Taylor J, Marincioni V, Korolija I, Altamirano H (2019) Evaluating retrofit options in a historical city center: Relevance of bio-based insulation and the need to consider complex urban form in decision-making. *Energy and Buildings* 182 196 - 204.

Cremades R, Sommer PS (2019) Computing climate-smart urban land use with the Integrated Urban Complexity model (IUCm 1.0). *Geoscientific Model Development* 12 525-539.

Dai E, Wu Z, Du X (2018) A gradient analysis on urban sprawl and urban landscape pattern between 1985 and 2000 in the Pearl River Delta, China. *Frontiers of Earth Science* 12 791-807.

Da-long L, Hui-hui Z, Jia-ping L (2019) Rule of long-wave radiation in enclosed building space. *Energy and Buildings* 182 311 - 321.

Demuzere M, Bechtel B, Mills G (2019) Global transferability of local climate zone models. *Urban Climate* 27 46–63.

Du WC, Xia XH (2018) How does urbanization affect GHG emissions? A cross-country panel threshold data analysis. *Applied Energy* 229 872-883.

Duarte RMBO, Piñeiro-Iglesias M, López-Mahía P, Muniategui-Lorenzo S, Moreda-Piñeiro J, Silva AMS, Duarte AC (2019) Comparative study of atmospheric water-soluble organic aerosols composition in contrasting suburban environments in the Iberian Peninsula Coast. *Science of The Total Environment* 648 430-441.

Dube T, Sibanda M, Bangamwabo V, Shoko C (2018) Establishing the link between urban land cover change and the proliferation of aquatic hyacinth (Eichhornia crassipes) in Harare Metropolitan, Zimbabwe. *Physics and Chemistry of the Earth*, Parts A/B/C 108 19-27.

Eeftens M, Odabasi D, Flückiger B, Davey M, Ineichen A, Feigenwinter C, Tsai M-Y (2019) Modelling the vertical gradient of nitrogen dioxide in an urban area. *Science of The Total Environment* 650 452-458.

Efthimiou GC (2019) Prediction of four concentration moments of an airborne material released from a point source in an urban environment. *Journal of Wind Engineering and Industrial Aerodynamics* 184 247–255.

Etuman AE, Coll I (2018) OLYMPUS v1.0: development of an integrated air pollutant and GHG urban emissions model - methodology and calibration over greater Paris. *Geoscientific Model Development* 11 5085-5111.

Evangelisti L, Guattari C, Asdrubali F (2019) On the sky temperature models and their influence on buildings energy performance: A critical review. *Energy and Buildings* 183 607 - 625.

Feng J, Li N, Zhang Z, Chen X (2018) How to apply the dependence structure analysis to extreme temperature and precipitation for disaster risk assessment. *Theoretical and Applied Climatology* 133(1-2) 297–305.

Fröhlich D, Gangwisch M, Matzarakis A (2019) Effect of radiation and wind on thermal comfort in urban environments - Application of the RayMan and SkyHelios model. *Urban Climate* 27 1 - 7.

Fu P, Weng Q (2018) Variability in annual temperature cycle in the urban areas of the United States as revealed by MODIS imagery. *ISPRS Journal of Photogrammetry and Remote Sensing* 146 65-73.

Fu P, Weng Q (2018) Responses of urban heat island in Atlanta to different land-use scenarios. *Theoretical and Applied Climatology* 133(1-2) 123–135.

Gabey AM, Grimmond CSB, Capel-Timms I (2019) Anthropogenic heat flux: advisable spatial resolutions when input data are scarce. *Theoretical and Applied Climatology* 135(1-2) 791–807.

Geirinhas JL, Trigo RM, Libonati R, Castro LCO, Sousa PM, Coelho CAS, Peres LF, de Avelar F.M. Magalhães M (2019) Characterizing the atmospheric conditions during the 2010 heatwave in Rio de Janeiro marked by excessive mortality rates. *Science of The Total Environment* 650 796-808.

Groma V, Ferenczi Z, Osán J, Török S, Steib R (2018) Verification of the EDMS model adapted to Budapest Liszt Ferenc Airport. *International Journal of Environment and Pollution* 63 137-153.

Gu B, Zhang X, Bai X, Fu B, Chen D (2019) Four steps to food security for swelling cities. *Nature* 566 31-33.

Guilbert A, Cremer KD, Heene B, Demoury C, Aerts R, Declerck P, Brasseur O, Nieuwenhuyse AV (2019) Personal exposure to traffic-related air pollutants and relationships with respiratory symptoms and oxidative stress: A pilot cross-sectional study among urban green space workers. *Science of The Total Environment* 649 620-628.

Hao L, Huang X, Qin M, Liu Y, Li W, Sun G (2018) Ecohydrological Processes Explain Urban Dry Island Effects in a Wet Region, Southern China. *Water Resources Research* 54 6757-6771.

Harshan S, Roth M, Velasco E, Demuzere M (2018) Evaluation of an urban land surface scheme over a tropical suburban neighborhood. *Theoretical and Applied Climatology* 133(3-4) 867–886.

Heo S, Bell M, Lee J-T (2019) Comparison of health risks by heat wave definition: Applicability of wet-bulb globe temperature for heat wave criteria. *Environmental Research* 168 158-170.

Herbel I, Croitoru AE, Rus AV, Roşca CF, Harpa GV, Ciupertealonuț AF, Rus I (2018) The impact of heat waves on surface urban heat island and local economy in Cluj-Napoca city, Romania. *Theoretical and Applied Climatology* 133(3-4) 681–695.

Hoan N, Liou Y, Nguyen K, Sharma R, Tran D, Liou C, Cham D (2018) Assessing the Effects of Land-Use Types in Surface Urban Heat Islands for Developing Comfortable Living in Hanoi City. *Remote Sensing* 10

Hou X, Chen L, Liu X, Li M, Shen Z (2019) Parameter transferability across spatial resolutions in urban hydrological modelling: a case study in Beijing, China. *Frontiers of Earth Science* 13 18-32.

Huang W-H, Chen B-Y, Kim H, Honda Y, Guo Y-L (2019) Significant effects of exposure to relatively low level ozone on daily mortality in 17 cities from three Eastern Asian Countries. *Environmental Research* 168 80-84.

Ielpo P, Mangia C, Marra GP, Comite V, Rizza U, Uricchio VF, Fermo P (2019) Outdoor spatial distribution and indoor levels of NO2 and SO2 in a high environmental risk site of the South Italy. *Science of The Total Environment* 648 787-797.

Ionov D, Poberovskii A (2019) Observations of urban NOx plume dispersion using mobile and satellite DOAS measurements around the megacity of St.Petersburg (Russia). *International Journal of Remote Sensing* 40 719-733.

Irmak MA, Yilmaz S, Mutlu E, Yilmaz H (2018) Assessment of the effects of different tree species on urban microclimate. *Environmental Science and Pollution Research* 25 15802-15822.

Ishida Y, Okaze T, Mochida A (2018) Influence of urban configuration on the structure of kinetic energy trans-

port and the energy dissipation rate. *Journal of Wind Engineering and Industrial Aerodynamics* 183 198–213.

Javanroodi K, Mandavinejad M, Nik VM (2018) Impacts of urban morphology on reducing cooling load and increasing ventilation potential in hot-arid climate. *Applied Energy* 231 714-746.

Jin K, Wang F, Yu Q, Gou J, Liu H (2018) Varied degrees of urbanization effects on observed surface air temperature trends in China. *Climate Research* 76 131-143.

Jing R, Wang M, Liang H, Wang X, Li N, Shah N, Zhao Y (2018) Multi-objective optimization of a neighborhood-level urban energy network: Considering Game-theory inspired multi-benefit allocation constraints. *Applied Energy* 231 534-548.

Kawaminami T, Ikegaya N, Hagishima A, Tanimoto J (2018) Velocity and scalar concentrations with low occurrence frequencies within urban canopy regions in a neutrally stable shear flow over simplified urban arrays. *Journal of Wind Engineering and Industrial Aerodynamics* 182 286–294.

Kent C, Grimmond S, Gatey D, Hirano K (2019) Urban morphology parameters from global digital elevation models: Implications for aerodynamic roughness and for wind-speed estimation. *Remote Sensing of Environment* 221 316-339.

Khan MF, Hamid AH, Bari MA, Tajudin ABA, Latif MT, Nadzir MSM, Sahani M, Wahab MIA, Yusup Y, Maulud KNA, Yusoff MF, Amin N, Akhtaruzzaman M, Kindzierski W, Kumar P (2019) Airborne particles in the city center of Kuala Lumpur: Origin, potential driving factors, and deposition flux in human respiratory airways. *Science of The Total Environment* 650 1195-1206.

Khansalari S, Raziei T, Mohebalhojeh AR, Ahmadi-Givi F (2018) Moderate to heavy cold-weather precipitation occurrences in Tehran and the associated circulation types. *Theoretical and Applied Climatology* 131(3-4) 985–1003.

Kohl L, Meng M, de Vera J, Bergquist B, Cooke CA, Hustins S, Jackson B, Chow CW, Chan AWH (2019) Limited Retention of Wildfire-Derived PAHs and Trace Elements in Indoor Environments. *Geophysical Research Letters* 46 383–391.

Kokkonen TV, Grimmond CSB, Christen A, Oke TR, Jarvi L (2018) Changes to the Water Balance Over a Century of Urban Development in Two Neighborhoods: Vancouver, Canada. *Water Resources Research* 54 6625-6642.

Kokogiannakis G, Darkwa J, Badeka S, Li Y (2019) Experimental comparison of green facades with outdoor test cells during a hot humid season. *Energy and Buildings* 185 196 - 209.

Krayenhoff ES, Moustaoui M, Broadbent AM, Gupta V, Georgescu M (2018) Diurnal interaction between urban expansion, climate change and adaptation in US cities. *Nature Climate Change* 8 1097+.

Lai J, Zhan W, Huang F, Voogt J, Bechtel B, Allen M, Peng S, Hong F, Liu Y, Du P (2018) Identification of typical diurnal patterns for clear-sky climatology of surface urban heat islands. *Remote Sensing of Environment* 217 203-220.

Lana X, Serra C, Casas-Castillo MC, Rodríguez-Solà R, Redaño A, Burgueño A (2018) Rainfall intensity patterns derived from the urban network of Barcelona (NE Spain). *Theoretical and Applied Climatology* 133(1-2) 385–403.

Leaf JS, Erell E (2018) A model of the ground surface temperature for micrometeorological analysis. *Theoretical and Applied Climatology* 133(3-4) 697–710.

Lee M, Hong T, Jeong K, Kim J (2018) A bottom-up approach for estimating the economic potential of the rooftop solar photovoltaic system considering the spatial and temporal diversity. *Applied Energy* 232 640-656.

Leibowicz BD, Lanham CM, Brozynski MT, Vazquez-Canteli JR, Castejon NC, Nagy Z (2018) Optimal decarbonization pathways for urban residential building energy services. *Applied Energy* 230 1311-1325.

Li H, Wang D, Cui L, Gao Y, Huo J, Wang X, Zhang Z, Tan Y, Huang Y, Cao J, Chow JC, Lee S-c, Fu Q (2019) Characteristics of atmospheric PM2.5 composition during the implementation of stringent pollution control measures in shanghai for the 2016 G20 summit. *Science of The Total Environment* 648 1121-1129.

Li H, Wolter M, Wang X, Sodoudi S (2018) Impact of land cover data on the simulation of urban heat island for Berlin using WRF coupled with bulk approach of Noah-LSM. *Theoretical and Applied Climatology* 134(1-2) 67–81.

Li H, Zhou Y, Wang X, Zhou X, Zhang H, Sodoudi S (2019) Quantifying urban heat island intensity and its physical mechanism using WRF/UCM. *Science of The Total Environment* 650 3110-3119.

Li J, Song G, Semakula HM, Zhang S (2019) Climatic burden of eating at home against away-from-home: A novel Bayesian Belief Network model for the mechanism of eating-out in urban China. *Science of The Total Environment* 650 224-232.

Li Q, Long R, Chen H (2018) Differences and influencing factors for Chinese urban resident willingness to pay for green housings: Evidence from five first-tier cities in China. *Applied Energy* 229 299-313.

Li R, Wang Z, Cui L, Fu H, Zhang L, Kong L, Chen W, Chen J (2019) Air pollution characteristics in China during 2015–2016: Spatiotemporal variations and key meteorological factors. *Science of The Total Environment* 648 902-915.

Li Y, Martinis S, Plank S, Ludwig R (2018) An automatic change detection approach for rapid flood mapping in

Sentinel-1 SAR data. I*nternational Journal of Applied Earth Observation and Geoinformation* 73 123-135.

Lima I, Scalco V, Lamberts R (2019) Estimating the impact of urban densification on high-rise office building cooling loads in a hot and humid climate. *Energy and Buildings* 182 30 - 44.

Limones-Rodríguez N, Marzo-Artigas J, Pita-López MF, Díaz-Cuevas MP (2018) The impact of climate change on air conditioning requirements in Andalusia at a detailed scale. *Theoretical and Applied Climatology* 134(3-4) 1047–1063.

Liu S, Su H, Tian J, Wang W (2018) An analysis of spatial representativeness of air temperature monitoring stations. *Theoretical and Applied Climatology* 132(3-4) 857–865.

Liu Y, Fang X, Xu Y, Zhang S, Luan Q (2018) Assessment of surface urban heat island across China's three main urban agglomerations. *Theoretical and Applied Climatology* 133(1-2) 473–488.

Livada I, Synnefa A, Haddad S, Paolini R, Garshasbi S, Ulpiani G, Fiorito F, Vassilakopoulou K, Osmond P, Santamouris M (2019) Time series analysis of ambient air-temperature during the period 1970–2016 over Sydney, Australia. *Science of The Total Environment* 648 1627-1638.

Luby IH, Polasky S, Swackhamer DL (2018) US Urban Water Prices: Cheaper When Drier. *Water Resources Research* 54 6126-6132.

Luo M, Lau NC (2018) Increasing Heat Stress in Urban Areas of Eastern China: Acceleration by Urbanization. *Geophysical Research Letters* 45 13060–13069.

Lyra A, Tavares P, Chou SC, Sueiro G, Dereczynski C. amd Sondermann M, Silva A (2018) Climate change projections over three metropolitan regions in Southeast Brazil using the non-hydrostatic Eta regional climate model at 5-km resolution. *Theoretical and Applied Climatology* 132(1-2) 663–682.

Matzarakis A, Fröhlich D, Bermon S, Adami PE (2018) Quantifying Thermal Stress for Sport Events-The Case of the Olympic Games 2020 in Tokyo. *Atmosphere* 9

Meng F, Li M, Cao J, Li J, Xiong M, Feng X, Ren G (2018) The effects of climate change on heating energy consumption of office buildings in different climate zones in China. *Theoretical and Applied Climatology* 133(1-2) 521–530.

Morakinyo TE, Lai A, Lau KK-L, Ng E (2019) Thermal benefits of vertical greening in a high-density city: Case study of Hong Kong. *Urban Forestry & Urban Greening* 37 42-55.

Moss JL, Doick KJ, Smith S, Shahrestani M (2019) Influence of evaporative cooling by urban forests on cooling demand in cities. *Urban Forestry & Urban Greening* 37 65-73.

Nandkeolyar N, Kiran S (2019) A climatological study of the spatio-temporal variability of land surface temperature and vegetation cover of Vadodara district of Gujarat using satellite data. *International Journal of Remote Sensing* 40 218-236.

Nastran M, Kobal M, Eler K (2019) Urban heat islands in relation to green land use in European cities. *Urban Forestry & Urban Greening* 37 33-41.

Nutkiewicz A, Jain RK, Bardhan R (2018) Energy modeling of urban informal settlement redevelopment: Exploring design parameters for optimal thermal comfort in Dharavi, Mumbai, India. *Applied Energy* 231 433-445.

Nutkiewicz A, Yang Z, Jain RK (2018) Data-driven Urban Energy Simulation (DUE-S): A framework for integrating engineering simulation and machine learning methods in a multi-scale urban energy modeling workflow. *Applied Energy* 225 1176-1189.

Omidvar H, Song J, Yang J, Arwatz G, Wang Z-H, Hultmark M, Kaloush K, Bou-Zeid E (2018) Rapid Modification of Urban Land Surface Temperature During Rainfall. *Water Resources Research* 54 4245-4264.

Papadopoulos S, Kontokosta CE (2019) Grading buildings on energy performance using city benchmarking data. *Applied Energy* 233 244-253.

Paralovo SL, Barbosa CGG, Carneiro IPS, Kurzlop P, Borillo GC, Schiochet MFC, Godoi AFL, Yamamoto CI, de Souza RAF, Andreoli RV, Ribeiro IO, Manzi AO, Kourtchev I, Bustillos JOV, Martin ST, Godoi RH (2019) Observations of particulate matter, NO2, SO2, O3, H2S and selected VOCs at a semi-urban environment in the Amazon region. *Science of The Total Environment* 650 996-1006.

Peng LLH, Yang X, He Y, Hu Z, Xu T, Jiang Z, Yao L (2019) Thermal and energy performance of two distinct green roofs: Temporal pattern and underlying factors in a subtropical climate. *Energy and Buildings* 185 247 - 258.

Perera ATD, Coccolo S, Scartezzini J-L, Mauree D (2018) Quantifying the impact of urban climate by extending the boundaries of urban energy system modeling. *Applied Energy* 222 847-860.

Pospieszyńska A, Przybylak R (2019) Air temperature changes in Toruń (central Poland) from 1871 to 2010. *Theoretical and Applied Climatology* 135(1-2) 707–724.

Qiu H, Yu H, Wang L, Zhu X, Chen M, Zhou L, Deng R, Zhang Y, Pu X, Pan J (2018) The burden of overall and cause-specific respiratory morbidity due to ambient air pollution in Sichuan Basin, China: A multi-city time-series analysis. *Environmental Research* 167 428-436.

Ramachandran S, Rajesh TA, Kedia S (2019) Influence of Relative Humidity, Mixed-Layer Height, and Mesoscale Vertical-Velocity Variations on Column and Surface

Aerosol Characteristics Over an Urban Region. *Boundary-Layer Meteorology* 170 161–181.

Ren C, Yang RZ, Cheng C, Xing P, Fang XY, Zhang S, Wang HF, Shi Y, Zhang XY, Kwok YT, Ng E (2018) Creating breathing cities by adopting urban ventilation assessment and wind corridor plan - The implementation in Chinese cities. *Journal of Wind Engineering and Industrial Aerodynamics* 182 170–188.

Rivas E, Santiago JL, Lechón Y, Martín F, Ariño A, Pons JJ, Santamaría JM (2019) CFD modelling of air quality in Pamplona City (Spain): Assessment, stations spatial representativeness and health impacts valuation. *Science of The Total Environment* 649 1362-1380.

Rodríguez-Algeciras J, Tablada A, Matzarakis A (2018) Effect of asymmetrical street canyons on pedestrian thermal comfort in warm-humid climate of Cuba. *Theoretical and Applied Climatology* 133(3-4) 663–679.

Rozbicka K, Rozbicki T (2018) Variability of UTCI index in South Warsaw depending on atmospheric circulation. *Theoretical and Applied Climatology* 133(1-2) 511–520.

Sadeghi SH, Hazbavi Z, Gholamalifard M (2019) Interactive impacts of climatic, hydrologic and anthropogenic activities on watershed health. *Science of The Total Environment* 648 880-893.

Salata F, Golasi I, Treiani N, Plos R, Vollaro A-d-L (2018) On the outdoor thermal perception and comfort of a Mediterranean subject across other Koppen-Geiger's climate zones. *Environmental Research* 167 115-128.

Salvati A, Monti P, Roura HC, Cecere C (2019) Climatic performance of urban textures: Analysis tools for a Mediterranean urban context. *Energy and Buildings* 185 162 - 179.

Santos LGR, Afshari A, Norford LK, Mao J (2018) Evaluating approaches for district-wide energy model calibration considering the Urban Heat Island effect. *Applied Energy* 215 31-40.

Saraga DE, Tolis EI, Maggos T, Vasilakos C, Bartzis JG (2019) PM2.5 source apportionment for the port city of Thessaloniki, Greece. *Science of The Total Environment* 650 2337-2354.

Sati AP, Mohan M (2018) The impact of urbanization during half a century on surface meteorology based on WRF model simulations over National Capital Region, India. Theoretical and Applied Climatology 134(1-2) 309–323.

Schloer H, Venghaus S, Hake J-F (2018) The FEW-Nexus city index - Measuring urban resilience. *Applied Energy* 210 382-392.

Shahid I, Chishtie F, Bulbul G, Shahid MZ, Shafique S, Lodhi A (2019) State of air quality in twin cities of Pakistan: Islamabad and Rawalpindi. *Atmósfera* 32 71-84.

Shi K, Chen Y, Li L, Huang C (2018) Spatiotemporal variations of urban CO2 emissions in China: A multiscale perspective. *Applied Energy* 211 218-229.

Sfîcă L, Ichim P, Apostol L, Ursu A (2018) The extent and intensity of the urban heat island in Iași city, Romania. *Theoretical and Applied Climatology* 134(3-4) 777–791.

Song S, Xu YP, Wu ZF, Deng XJ, Wang Q (2019) The relative impact of urbanization and precipitation on long-term water level variations in the Yangtze River Delta. *Science of The Total Environment* 648 460-471.

Sosa-Echeverría R, Alarcón-Jiménez AL, Torres-Barrera MdC, Jaimes-Palomera M, Retama-Hernández A, Sánchez-Álvarez P, Granados-Hernández E, Bravo-Álvarez H (2019) Spatial and temporal variation of acid rain in the Mexico City Metropolitan Zone. *Atmósfera* 32 55-69.

Spentzou E, Cook MJ, Emmitt S (2019) Modelling natural ventilation for summer thermal comfort in Mediterranean dwellings. *International Journal of Ventilation* 18 28-45.

Staiger H, Laschewski G, Matzarakis A (2019) Selection of Appropriate Thermal Indices for Applications in Human Biometeorological Studies. *Atmosphere* 10

Sun J, Shen Z, Zhang L, Lei Y, Gong X, Zhang Q, Zhang T, Xu H, Cui S, Wang Q, Cao J, Tao J, Zhang N, Zhang R (2019) Chemical source profiles of urban fugitive dust PM2.5 samples from 21 cities across China. *Science of The Total Environment* 649 1045-1053.

Taibi S, Meddi M, Mahe G (2019) Seasonal rainfall variability in the southern Mediterranean border: Observations, regional model simulations and future climate projections. *Atmósfera* 32 39-54.

Takadate Y, Uematsu Y (2019) Design wind wind force coefficients for the main wind force resisting systems of open- and semi-open-type framed membrane structures with gable roofs. *Journal of Wind Engineering and Industrial Aerodynamics* 184 265–276.

Toparlar Y, Blocken B, Maiheu B, van Heijst GJF (2018) Impact of urban microclimate on summertime building cooling demand: A parametric analysis for Antwerp, Belgium. *Applied Energy* 228 852-872.

Ullah H, Rashid A, Liu G, Hussain M (2018) Perceptions of mountainous people on climate change, livelihood practices and climatic shocks: A case study of Swat District, Pakistan. *Urban Climate* 26 244 - 257.

Velázquez-Gómez M, Hurtado-Fernández E, Lacorte S (2019) Differential occurrence, profiles and uptake of dust contaminants in the Barcelona urban area. *Science of The Total Environment* 648 1354-1370.

Vera S, Pinto C, Tabares-Velasco PC, Bustamante W (2018) A critical review of heat and mass transfer in vegetative roof models used in building energy and urban environment simulation tools. *Applied Energy* 232 752-764.

Verdonck M-I, Demuzere M, Bechtel B, Beck C, Brousse O, Droste A, Fenner D, Leconte F, Van Coillie F (2019) The Human Influence Experiment (Part 2): Guidelines for Improved Mapping of Local Climate Zones Using a Supervised Classification. *Urban Science* 3 27.

Vlastos D, Antonopoulou M, Lavranou A, Efthimiou I, Dailianis S, Hela D, Lambropoulou D, Paschalidou AK, Kassomenos P (2019) Assessment of the toxic potential of rainwater precipitation: First evidence from a case study in three Greek cities. *Science of The Total Environment* 648 1323-1332.

de Vos LW, Raupach TH, Leijnse H, Overeem A, Berne A, Uijlenhoet R (2018) High-Resolution Simulation Study Exploring the Potential of Radars, Crowdsourced Personal Weather Stations, and Commercial Microwave Links to Monitor Small-Scale Urban Rainfall. *Water Resources Research* 54 10293-10312.

Voulis N, Warnier M, Brazier FMT (2018) Understanding spatio-temporal electricity demand at different urban scales: A data-driven approach. *Applied Energy* 230 1157-1171.

Wang X, Yin Z, Wang X, Tian P, Huang Y (2018) A study on flooding scenario simulation of future extreme precipitation in Shanghai. Frontiers of Earth Science 12 834-845.

Wang Y, Xue Z, Chen J, Chen G (2019) Spatio-temporal analysis of phenology in Yangtze River Delta based on MODIS NDVI time series from 2001 to 2015. *Frontiers of Earth Science* 13 92-110.

Weng Q, Firozjaei MK, Kiavarz M, Alavipanah SK, Hamzeh S (2019) Normalizing land surface temperature for environmental parameters in mountainous and urban areas of a cold semi-arid climate. *Science of The Total Environment* 650 515-529.

Wolfe P, Davidson K, Fulcher C, Fann N, Zawacki M, Baker KR (2019) Monetized health benefits attributable to mobile source emission reductions across the United States in 2025. *Science of The Total Environment* 650 2490-2498.

Wu D, Lin JC, Fasoli B, Oda T, Ye X, Lauvaux T, Yang EG, Kort EA (2018) A Lagrangian approach towards extracting signals of urban CO2 emissions from satellite observations of atmospheric column CO2 (XCO2): X-Stochastic Time-Inverted Lagrangian Transport model ("X-STILT v1"). *Geoscientific Model Development* 11 4843-4871.

Wu W, Li Q, Zhang Y, Du X, Wang H (2018) Two-Step Urban Water Index (TSUWI): A New Technique for High-Resolution Mapping of Urban Surface Water. *Remote Sensing* 10

Xia H, Chen Y, Quan J (2018) A simple method based on the thermal anomaly index to detect industrial heat sources. International *Journal of Applied Earth Observation and Geoinformation* 73 627-637.

Xing Q, Hao X, Lin Y, Tan H, Yang K (2019) Experimental investigation on the thermal performance of a vertical greening system with green roof in wet and cold climates during winter. *Energy and Buildings* 183 105 - 117.

Xu H-J, Yang X-R, Li S, Xue X-M, Chang S, Li H, Singh BK, Su J-Q, Zhu Y-G (2019) Nitrogen inputs are more important than denitrifier abundances in controlling denitrification-derived N2O emission from both urban and agricultural soils. Science of The Total Environment 650 2807-2817.

Xu X, Gonzalez JE, Shen S, Miao S, Dou J (2018) Impacts of urbanization and air pollution on building energy demands - Beijing case study. *Applied Energy* 225 98-109.

Xu Z, FitzGerald G, Guo Y, Jalaludin B, Tong S (2019) Assessing heatwave impacts on cause-specific emergency department visits in urban and rural communities of Queensland, Australia. *Environmental Research* 168 414-419.

Yamamoto M, Kasai M, Okaze T, Hanaoka K, Mochida A (2018) Analysis of climatic factors leading to future summer heatstroke risk changes in Tokyo and Sendai based on dynamical downscaling of pseudo global warming data using WRF. *Journal of Wind Engineering and Industrial Aerodynamics* 183 187–197.

Yan J, Feng J-C (2018) Visual special issue: Low carbon development and transformation of cities. *Applied Energy* 231 A1-A3.

Yan X, Li Z, Luo N, Shi W, Zhao W, Yang X, Liang C, Zhang F, Cribb M (2019) An improved algorithm for retrieving the fine-mode fraction of aerosol optical thickness. Part 2: Application and validation in Asia. *Remote Sensing of Environment* 222 90-103.

Yang J, Yin P, Sun J, Wang B, Zhou M, Li M, Tong S, Meng B, Guo Y, Liu Q (2019) Heatwave and mortality in 31 major Chinese cities: Definition, vulnerability and implications. *Science of The Total Environment* 649 695-702.

Yang J, Zhang Z, Li X, Xi J, Feng Z (2018) Spatial differentiation of China's summer tourist destinations based on climatic suitability using the Universal Thermal Climate Index. *Theoretical and Applied Climatology* 134(3-4) 859–874.

Yao R, Cao J, Wang L, Zhang W, Wu X (2019) Urbanization effects on vegetation cover in major African cities during 2001-2017. *International Journal of Applied Earth Observation and Geoinformation* 75 44-53.

Yeo I-A, Lee E (2018) Quantitative study on environment and energy information for land use planning scenarios in eco-city planning stage. *Applied Energy* 230 889-911.

Yildiz ND, Avdan U, Yilmaz S, Matzarakis A (2018) Thermal map assessment under climate and land use changes; a case study for Uzundere Basin. *Environmental Science*

and Pollution Research 25 940-951.

Yilmaz S, Mutlu E, Yilmaz H (2018) Alternative scenarios for ecological urbanizations using ENVI-met model. *Environmental science and pollution research* 25 26307-26321.

You S, Lim YJ, Dai Y, Wang C-H (2018) On the temporal modelling of solar photovoltaic soiling: Energy and economic impacts in seven cities. *Applied Energy* 228 1136-1146.

Yu Q, Acheampong M, Pu R, Landry S, Ji W, Dahigamuwa T (2018) Assessing effects of urban vegetation height on land surface temperature in the City of Tampa, Florida, USA. *International Journal of Applied Earth Observation and Geoinformation* 73 712-720.

Zanforlin S, Letizia S (2019) Effects of upstream buildings on the performance of a synergistic roof-and-diffuser augmentation system for cross flow wind turbines. *Journal of Wind Engineering and Industrial Aerodynamics* 184 329–341.

Zhang D, Zhang Q, Qi S, Huang J, Karplus VJ, Zhang X (2019) Integrity of firms' emissions reporting in China's early carbon markets. *Nature Climate Change* 9 164+.

Zhang S, Huang G, Qi Y, Jia G (2018) Impact of urbanization on summer rainfall in Beijing–Tianjin–Hebei metropolis under different climate backgrounds. *Theoretical and Applied Climatology* 133(3-4) 1093–1106.

Zhang W, Tong S, Ge M, An J, Shi Z, Hou S, Xia K, Qu Y, Zhang H, Chu B, Sun Y, He H (2019) Variations and sources of nitrous acid (HONO) during a severe pollution episode in Beijing in winter 2016. *Science of The Total Environment* 648 253-262.

Zhang W, Villarini G, Vecchi GA, Smith JA (2018) Urbanization exacerbated the rainfall and flooding caused by hurricane Harvey in Houston. *Nature* 563 384+.

Zhang Y, Sun L (2019) Spatial-temporal impacts of urban land use land cover on land surface temperature: Case studies of two Canadian urban areas. International *Journal of Applied Earth Observation and Geoinformation* 75 171-181.

Zhao D, Wu J (2018) Changes in urban-related precipitation in the summer over three city clusters in China. *Theorethical and Applied Climatology* 134(1-2) 83–93.

Zhao L (2018) Urban growth and climate adaptation. *Nature Climate Change* 8 1034.

Zheng XW, Li HN, Li C (2019) Damage probability analysis of a high-rise building against wind excitation with recorded field data and direction effect. *Journal of Wind Engineering and Industrial Aerodynamics* 184 10–22.

Zhou TN, Wang XH, He JJ, Chen QP, Wang J (2019) The effect of forced ventilation by using two movable fans on thermal smoke movement in a tunnel fire. *Journal of Wind Engineering and Industrial Aerodynamics* 184 321–328.

Zhu P, Yan D, Sun H, An J, Huang Y (2019) Building Blocks Energy Estimation (BBEE): A method for building energy estimation on district level. *Energy and Buildings* 185 137 - 147.

Zinzi M, Carnielo E, Mattoni B (2018) On the relation between urban climate and energy performance of buildings. A three-years experience in Rome, Italy. *Applied Energy* 221 148-160.

Zullo F, Fazio G, Romano B, Marucci A, Fiorini L (2019) Effects of urban growth spatial pattern (UGSP) on the land surface temperature (LST): A study in the Po Valley (Italy). *Science of The Total Environment* 650 1740-1751.

Zuo S, Dai S, Song X, Xu C, Liao Y, Chang W, Chen Q, Li Y, Tang J, Man W, Ren Y (2018) Determining the Mechanisms that Influence the Surface Temperature of Urban Forest Canopies by Combining Remote Sensing Methods, Ground Observations, and Spatial Statistical Models. *Remote Sensing* 10

Žuvela-Aloise M, Andre K, Schwaiger H., Bird DN, Gallaun H (2018) Modelling reduction of urban heat load in Vienna by modifying surface properties of roofs. *Theorethical and Applied Climatology* 131(3-4) 1005–1018.

Journal Special Issue

Announcing a special issue of the journal *Geography, Environment and Sustainability* on "Urban environmental geography: Moscow and other megacities"

https://ges.rgo.ru/jour/pages/view/special

Guest editors:
1) Dr. Prof. N. Chubarova
2) Dr. Prof. N. Kosheleva
3) Dr. C. Calfapietra
4) Dr. V. Vasenev
5) Dr. Prof. Z. Cheng
6) Dr. Prof. J.L. Morel

The topics of the special issue include:

- *Snow, soil and road dust as geochemical indicators of the megacity environment;*
- *Urban air pollution and meteorological processes;*
- *Urban hydrological systems – water quality and river ecology;*
- *Urbanization and quality of life;*
- *Urban green infrastructure.*

Deadline: June 15th, 2019

Upcoming Conferences...

WEBINAR SERIES ON "PASSIVE AIR POLLUTION MITIGATION IN THE BUILT ENVIRONMENT"
Sponsored by Trinity College Dublin, Cornell University, and the U.S. Environmental Protection Agency • March 28, 2019 (see link for future monthly dates)
https://www.tcd.ie/civileng/air-pollution-webinar-series/

EUROPEAN GEOSCIENCES UNION (EGU) GENERAL ASSEMBLY SESSION: "URBAN CLIMATE, URBAN BIOMETEOROLOGY, AND SCIENCE TOOLS FOR CITIES"
Vienna, Austria • April 7–12 2019
https://www.egu2019.eu

WORKSHOP ON OPEN-GROWN AND URBAN TREES 2019
Freiburg, Germany • April 7-10, 2019
https://www.meteo.uni-freiburg.de/en/events/workshop-on-open-grown-and-urban-trees-2019

COMFORT AT THE EXTREMES: ENERGY, ECONOMY AND CLIMATE (CATE)
Dubai • April 10-11, 2019
https://comfortattheextremes.com

JOINT URBAN REMOTE SENSING EVENT (JURSE)
Vannes, France • May 22-24, 2019
http://www.jurse2019.org

ENERGY AND SOCIETY IN TRANSITION: 2ND INTERNATIONAL CONFERENCE ON ENERGY RESEARCH AND SOCIAL SCIENCE
Tempe, Arizona USA • May 28-31, 2019
https://www.elsevier.com/events/conferences/international-conference-on-energy-research-and-social-science

INTERNATIONAL CONFERENCE ON SUSTAINABILITY IN ENERGY AND BUILDINGS (SEB-19)
Budapest, Hungary • July 4-5, 2019
http://seb-19.kesinternational.org/

The **ICOS WORKSHOP ON STRATEGIES TO MONITOR GREENHOUSE GASES IN URBAN ENVIRONMENTS** will be held July 1-4, 2019, in Helsinki and at the Hyytiälä station in Finland.

Cities are hot spots for anthropogenic greenhouse gas emissions. Developing methods to monitor and validate the GHG emissions in them is critical to fulfill the UN Paris and Katowice Agreements.

The goal of the ICOS workshop is to define measurement needs and goals, discuss and address challenges of urban monitoring, and work towards a comprehensive roadmap for embedding urban measurements in a coherent and standardised effort within the long-term observation infrastructure of ICOS, considering also how this can contribute to and integrate with other organisations and networks, such as WMO IG3IS.

The workshop is limited to 20 – 25 participants. Accommodation and food will be approximately 255 euros/person in a double and 285 euros/person in a single room. The food covers breakfast, lunch, dinner and evening snack. Registration closes April 15, 2019 (https://www.icos-ri.eu/event/471).

OCEANIA GEOSCIENCES SOCIETY (AOGS) SESSION ON "ROLE OF URBANIZATION ON WEATHER AND CLIMATE OF CITIES"
Singapore • July 28-August 2, 2019
http://www.asiaoceania.org/society/index.asp

EUROPEAN METEOROLOGICAL SOCIETY SESSION ON "INTERACTIONS OF AIR POLLUTANTS, GREENHOUSE GASES, WEATHER AND CLIMATE FROM LOCAL/URBAN TO GLOBAL SCALES"
Copenhagen, Denmark • September 9-13, 2019
https://meetingorganizer.copernicus.org/EMS2019/session/33616

SYMPOSIUM ON CHALLENGES FOR APPLIED HUMAN BIOMETEOROLOGY, ALBERT-LUDWIGS-UNIV.
Freiburg, Germany • March 2-3, 2020
https://www.medizin-meteorologie.de/index.php/16-register

CALL FOR PAPERS: *PLOS ONE*, on the theme of "Urban Ecosystems," invites submissions spanning the intersection of ecological, climatological, and sociological patterns and processes within urban systems. Submission are due by July 12, 2019.
https://collections.plos.org/s/urban-ecosystems

Sydney, Australia selected to host ICUC-11 in 2021

The next International Conference on Urban Climate **(ICUC-11)** will take place in **Sydney, Australia from August 30 to September 3, 2021**. The Board of the International Association for Urban Climate (IAUC) selected the team in Sydney with its proposal "Cities as Living Labs: Climate, Vulnerability, and Multidisciplinary Solutions" on April 4, 2019. The Board's decision follows the results of a membership consultation in March. In the membership consultation, a strong preference for Sydney emerged. From a total of 240 voters, 64% ranked Sydney their first choice, followed by 19% that ranked "Hong Kong" first and 17% that ranked "Beijing" first.

The University of New South Wales (UNSW) who will host ICUC-11 has also received support from the American Meteorological Society (AMS) Board on the Urban Environment (BUE) to run ICUC-11 together with the Symposium on the Urban Environment (AMS-BUE). UNSW will collaborate with other Australian Universities and Research Institutes in hosting this conference. Dr. Negin Nazarian, who leads the organising committee, welcomes the IAUC community to Sydney: "We greatly appreciate the vote of confidence from the IAUC members. We truly believe that Sydney is an ideal venue for bringing in the diverse and international Urban Climate community, and look forward to welcoming all members in Sydney, Australia, for the 11th International Conference on Urban Climate (ICUC-11) in 2021."

ICUC-11 will be hosted on the campus of UNSW. The Sir John Clancy auditorium offers tiered seating for up to 945 participants in plenary sessions. The adjacent Matthews Pavillions will provide a contemporary semi-enclosed space for exhibitions, poster display and catering. A number of nearby theatres and lecture rooms will offer spaces for concurrent sessions and workshops.

The board congratulates the team from Sydney which will make a highly attractive venue for our flagship meeting. The board also greatly appreciates the work and willingness by all candidate teams to host ICUC-11, including Beijing and Hong Kong who each developed very attractive proposals, but were ultimately unsuccessful.

Call for nominations – 2019 Luke Howard Award

The IAUC is pleased to announce the call for nominations for the 2019 'Luke Howard Award for Outstanding Contributions to the Field of Urban Climatology.'

The Luke Howard Award may be given annually to an individual who has made **outstanding contributions to the field of urban climatology** in a combination of **research, teaching, and/or service** to the international community of urban climatologists.

The IAUC is committed to promoting equality and diversity. Therefore we particularly encourage nominations for suitable candidates from under-represented groups.

The person making the nomination will act as the coordinator to put together a nomination package (including a CV of the nominee and three letters of recommendation). Self-nominations are not permitted and current Awards Committee members cannot be evaluated. Complete nomination packages should be submitted (as a single electronic submission) to the IAUC Awards Committee Chair, **Dr. Helen Ward**: helen.ward@uibk.ac.at

Luke Howard Award Nomination Process

• Inform the Awards Committee Chair of the intent to nominate an individual. The intent to nominate should be communicated via email to the Awards Committee Chair by **24 May, 2019**;

• Nomination materials should be collected by the coordinator (i.e. the person notifying the Awards Committee Chair that a particular individual will be nominated);

• The coordinator should collect the following documentation:

a) a three-page candidate CV

b) three letters of recommendation (two pages in length) from IAUC members from at least two different countries;

• Complete packages should reach the Awards Committee Chair by **30 June, 2019**.

The IAUC Awards committee will then recommend the name of a recipient for consideration and approval by the IAUC Board. Nominations will be active for three years, and updated information may be submitted for consideration in the second and third years. Currently there are no active nominations remaining so we strongly encourage members to nominate suitable candidates for the 2019 Award.

Previous winners of the Luke Howard Award include:

- 2018 Prof. Dr. Wilhelm Kuttler, University of Duisburg-Essen, Germany
- 2016 Dr. Walter Dabberdt, Vaisala Group, USA
- 2015 Prof. Emeritus Anthony Brazel, Arizona State University, USA
- 2014 Prof. Manabu Kanda, Tokyo Institute of Technology, Japan
- 2013 Professor Emeritus Yair Goldreich, Bar-Ilan University, Israel
- 2010 Professor John Arnfield, The Ohio State University, USA
- 2009 Professor Sue Grimmond, King's College, UK
- 2008 Professor Bob Bornstein, San José State University, USA
- 2007 Professor (Emeritus) Masatoshi Yoshino, University of Tsukuba, Japan
- 2006 Professor Arieh Bitan, Tel Aviv University, Israel
- 2005 Professor Ernesto Jauregui, UNAM, Mexico
- 2004 Professor Tim Oke, UBC, Canada

IAUC Board Members & Terms

- **President**: Nigel Tapper (Monash University, Australia), 2018-2022.
- **Secretary**: Andreas Christen (Albert-Ludwigs Universität Freiburg, Germany), 2018-2022.
- **Treasurer**: Ariane Middel (Temple University, USA), 2019-2022.
- Alexander Baklanov (WMO, Switzerland), *WMO Representative*, 2018-2022.**
- Benjamin Bechtel (Universität Hamburg, Germany), 2017-2021.
- Matthias Demuzere (Kode, Belgium), 2019-2022.
- Jorge Gonzalez (CUNY, USA): *ICUC10 Local Organizer*, 2016-2021.
- Aya Hagishima (Kyushu University, Japan), 2015-2019.
- Leena Järvi (University of Helsinki, Finland), 2016-2020.
- Dev Niyogi (Purdue University, USA): *ICUC10 Local Organizer*, 2016-2021.
- David Pearlmutter (Ben-Gurion University, Israel), *Newsletter Editor*, 2008-*
- Chao Ren (University of Hong Kong, Hong Kong), 2017-2021.
- David Sailor (Arizona State University, USA), *Past Secretary* 2014-2018.*
- James Voogt (University of Western Ontario, Canada), *Past President*: 2014-2018.*
- Helen Ward (University of Innsbruck, Austria), 2019-2022.

* non-voting, ** non-voting appointed member

IAUC Committee Chairs

- **Editor, IAUC Newsletter**: David Pearlmutter
  - News Editor: Paul Alexander
  - Urban Projects Editor: Helen Ward
  - Conferences Editor: Joe McFadden
- **Bibliography Committee**: Matthias Demuzere
- **Chair Teaching Resources**: Gerald Mills
- **Chair Awards Committee**: Nigel Tapper

Urban Climate News – The Quarterly Newsletter of the International Association for Urban Climate

Editor: David Pearlmutter
davidp@bgu.ac.il

Urban Projects: Helen Ward
Helen.Ward@uibk.ac.at

News: Paul Alexander
paul.alexander@cso.ie

Conferences: Joe McFadden
mcfadden@ucsb.edu

The next edition of ***Urban Climate News*** will appear in late June. Contributions for the upcoming issue are welcome, and should be submitted by May 31, 2019 to the relevant editor.

Submissions should be concise and accessible to a wide audience. The articles in this Newsletter are unrefereed, and their appearance does not constitute formal publication; they should not be used or cited otherwise.

Bibliography: Matthias Demuzere and BibCom members
Matthias.demuzere@rub.de